FUNCTIONAL CHACRATERISTICS ENHANCEMENT OF AUSTENITIC STAINLESS STEEL (SS-316 L) THROUGH MICROWAVE HYBRID HEATING

A Thesis submitted in the fulfillment of the requirement for the award of the degree of

MASTER OF ENGINEERING

IN

PRODUCTION ENGINEERING

Submitted by

DILKARAN SINGH

Roll No. 801685005

Under the supervision of

Dr. Dheeraj Gupta
Associate Professor
MED, TIET, Patiala

Dr. Vivek Jain
Associate Professor
MED, TIET, Patiala

MECHANICAL ENGINEERING DEPARTMENT

THAPAR INSTITUTE OF ENGINEERING AND TECHNOLOGY,

PATIALA-147004, INDIA

(Declared as Deemed-to-be University u/s of the UGC Act, 1956 Vide Notification No. F9-12-84-U.3 of G.O.I)

June 2018

CERTIFICATE

I, Dilkaran Singh, Roll. No. 801685005, hereby declares that the thesis entitled **"Functional Characteristics Enhancement of Austenitic Stainless Steel (SS-316 L) Through Microwave Hybrid Heating"** submitted to the Department of Mechanical Engineering at Thapar Institute of Engineering & Technology, Patiala, Punjab, for the award of the degree of **Master of Engineering**, is a record of original bonafide research work carried out by me under the supervision of **Dr. Dheeraj Gupta** and **Dr. Vivek Jain**. All the requirements for the submission of this thesis have been fulfilled as per institute norms.

The results presented in this thesis have not been submitted elsewhere for the award of a degree or diploma.

Dilkaran Singh 26/07/18

Dilkaran Singh

Roll. No. 801685005

26/07/18

Dr. Dheeraj Gupta

Associate Professor

Department of Mechanical Engineering

TIET, Patiala-147004

26/7/18

Dr. Vivek Jain

Associate Professor

Department of Mechanical Engineering

TIET, Patiala-147004

Date:

Place: Thapar Institute of Engineering & Technology, Patiala-147004, Punjab, India.

Dedicated to

My Parents

ACKNOWLEDGEMENT

First and foremost, I wish to thank my supervisors **Dr. Dheeraj Gupta** and **Dr. Vivek Jain** for their valuable support, supervision, guidance and belief in me. I am thankful for the positive suggestions, and meticulous guidance that helped me to improve my scientific writing and carry out the new research. I feel really motivated and honoured to work under their guidance throughout my entire M.E thesis work.

A special thanks to the office of Mechanical Engineering Department for providing all the facilities required for research work. Thanks to all my lab mates, colleagues and friends for their support and a very special and sincere thanks to Mr. Sarbjeet Kaushal who had helped me a lot during my research work. I am thankful to the office staff of the ME department at Thapar Institute of Engineering & Technology for their help and cooperation throughout my study.

A huge thanks goes to my parents, Mr. Jagtar Singh and Mrs. Kanwarjeet Kaur, who always encouraged me and stood by me. I thank all my family and relatives who had supported and cared for me during my research work. I wish to thank all those who have helped me directly or indirectly in this journey of my life.

Finally, I bow and thank the Almighty, without whom I could have not completed this journey of completing my research work.

Dilkaran Singh

ABSTRACT

The primary objective of the present study was to develop a wear resistant cladding on austenitic stainless steel (SS-316 L) substrate through microwave hybrid heating technique. Austenitic stainless steel is widely used in almost every manufacturing industries. This can be attributed to their exceptional corrosion resistance. However, this grade of stainless steel are deprived of wear resistance properties when exposed under severe wear working conditions. The failure of these materials cause huge economical loss to developing countries like India. The wear performance of austenitic stainless steel can be improved by coating/cladding the surface of steels with wear resistant materials. Microwave energy has emerged as a novel material processing technique in the past years. The clads of Ni-based20WC8Co-10Mo and Ni-based10WC8Co-10Cr3C2 powder compositions were successfully developed on austenitic stainless steel (SS-316 L) substrate using multimode domestic microwave oven working at frequency of 2.45 GHz. Microwave exposure time and power level were selected as the process parameters. The process parameters were optimized to get good metallurgically bonded clads. The developed clads were further characterized through various relevant techniques like scanning electron microscope (SEM), energy dispersive spectroscopy (EDS), X-ray diffraction (XRD), dry sliding wear test, Vickers microhardness test and flexural strength test.The SEM images revealed the thickness of the developed clads to be 1 mm approximately. The developed clads were free from any type of cracks and porosity. The presence of Fe in the clad region supported and verified the claim of metallurgical bonding between the clad and substrate. The magnified image of the clad region showed the presence of hard carbide particles randomly distributed in the clad region. These hard carbide particles were responsible for increasing the microhardness value of the developed clads which was measured to be 503 ± 34 Hv for Ni-based10WC8Co-10Cr3C2 clad and 752 ± 34 Hv for Ni-based20WC8Co-10Mo clad.

TABLE OF CONTENTS

LIST OF FIGURES

LIST OF TABLES

LIST OF ABBREVIATIONS

CVD	:	Chemical Vapor Deposition
Cr_3C_2	:	Chromium Carbide
EDS	:	Energy Dispersive X-ray Spectroscopy
EM	:	Electro Magnetic
MHH	:	Microwave Hybrid Heating
MHz	:	Mega Hertz
Mo	:	Molybdenum
MPa	:	Mega Pascal
MS	:	Mild Steel
MW	:	Microwave
OM	:	Optical Micrograph
SEM	:	Scanning Electron Microscopy
SS	:	Stainless Steel
WC	:	Tungsten Carbide
XRD	:	X-ray Diffraction

Chapter 1
Introduction

1.1 Stainless Steel

Stainless steel is a family of corrosion resistant steel alloys containing at least 10.5% of chromium [1]. They have high resistance to corrosion because of formation of naturally occurring chromium-rich oxide layer on the surface of the steel which is extremely thin and invisible. Iron is the dominant component of stainless steel mixed with other elements like chromium, nickel, silicon, molybdenum, aluminium, and carbon. There are greater than 57 stainless steel types which are identified as standard alloys and some of them are shown in figure 1.1. All these types of stainless steels are used in a numerous number of applications and industries: automobile components, cutlery, and kitchenware, power generation, food production and storage, building and construction, medical applications, oil and gas industries, marine and shipbuilding, just to name a few.

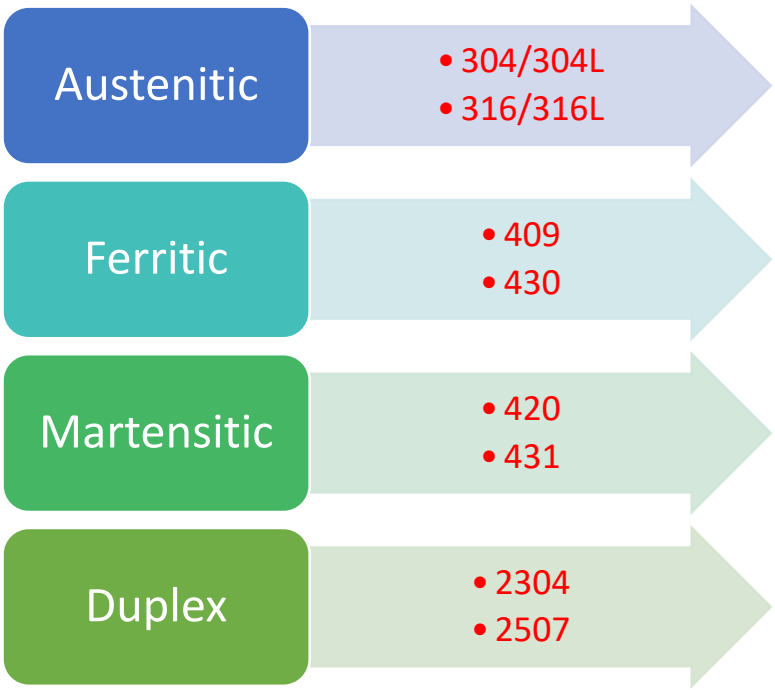

Figure 1.1: Different grades of stainless steel

1.2 Surface Engineering

Surface engineering is the spectrum of all the engineering applications and is one of the key methods for overcoming wear, corrosion, frictional energy loses, high temperature oxidation, etc. It is used to modify the properties of the surface of engineering components to extend the life and serviceability of components. Surface engineering is defined as a technology which is designed to alter the properties of the surface of metallic and non-metallic constituents to be used for functional or decorative purposes. The surface of a material and surface contact area vastly determine the behavior of the material. The surface of an engineering component is made up of a matrix of individual grains consisting of varying grain size and bond strength depending on the process by which the component was manufactured, and on the elements which was used to form those grains. One of the major properties required by engineering components is shown in figure 1.2.

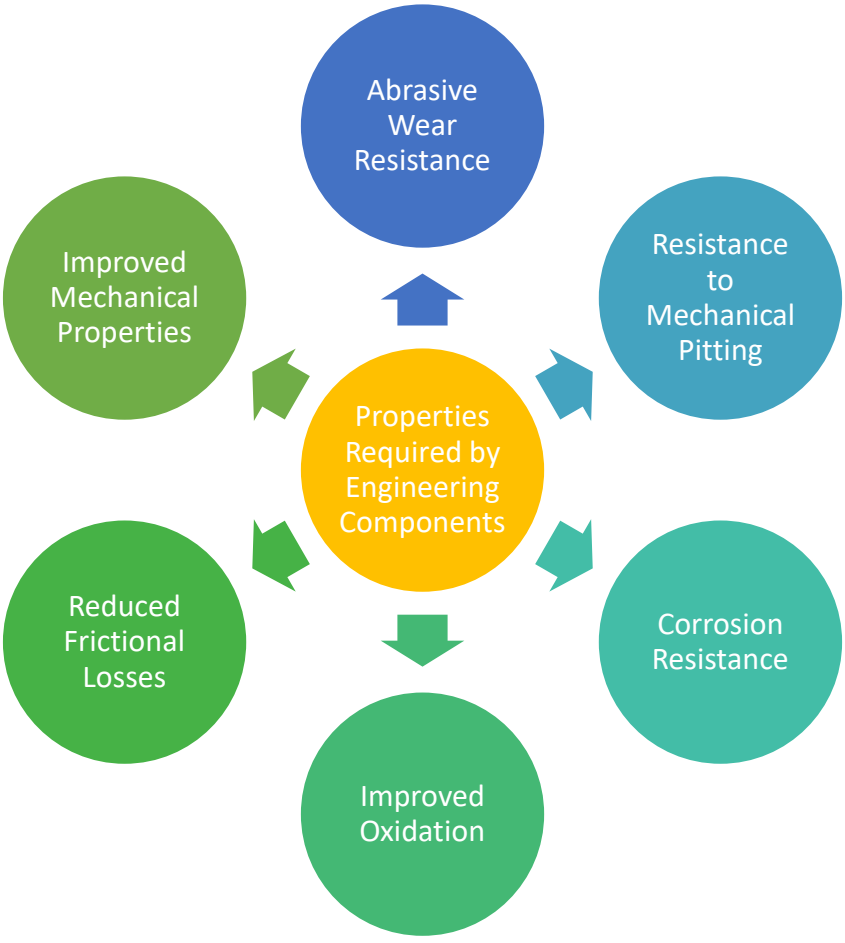

Figure 1.2: Desired properties of surface engineering components

There are two approaches to design the engineering components for longer life- first, substituting the material with better one, and second, surface modification of the material by coating less wear resistive component with the high resistive material. The second approach is more realistic and economical as wear and corrosion are known to be surface related phenomena. Different types of surface engineering options are shown in figure 1.3.

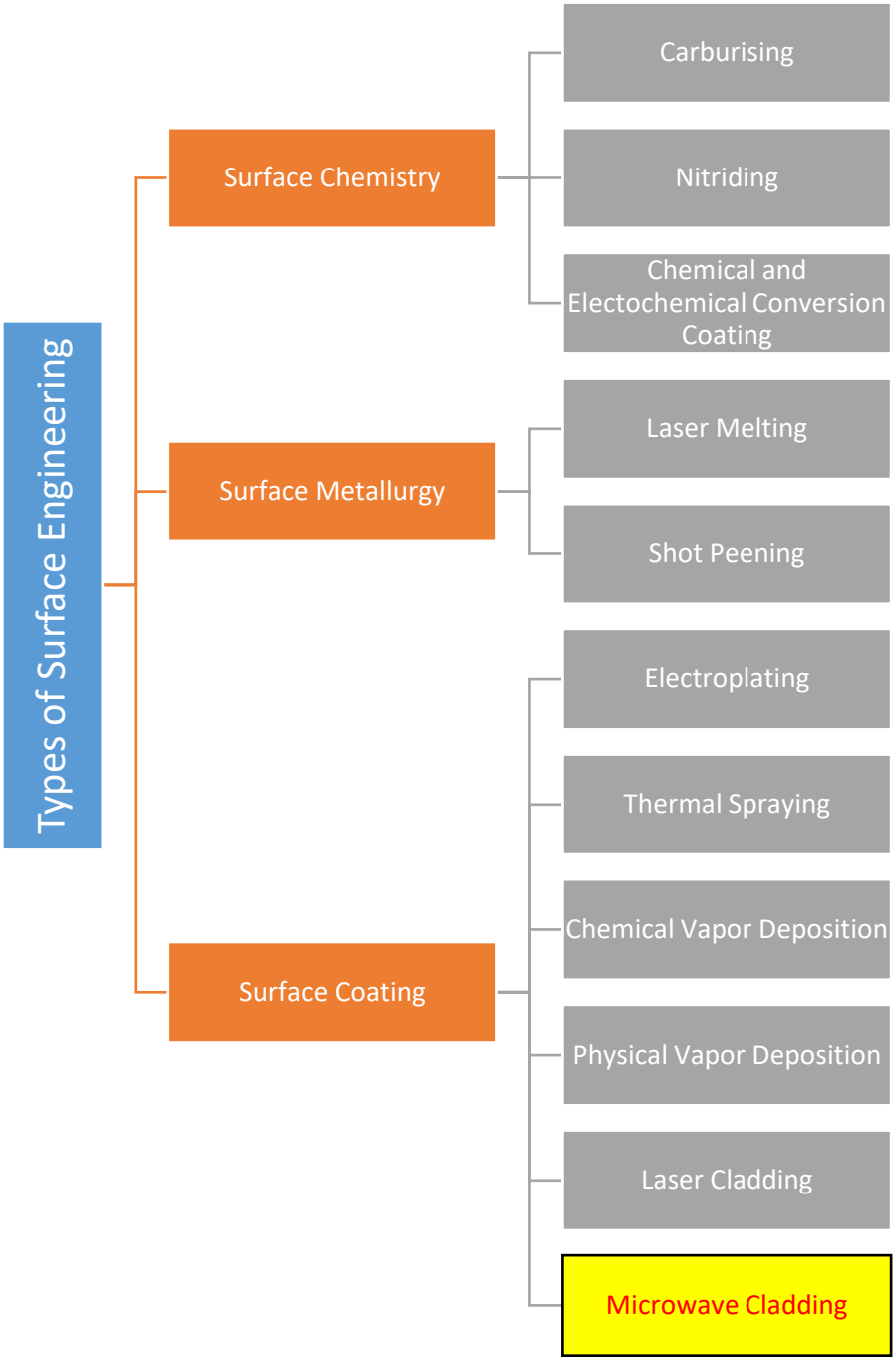

Figure 1.3: Types of surface engineering processes

1.3 Surface Coating

Surface coating is the process in which a substance is applied to other material in order to change its surface properties while keeping the bulk properties unchanged. The successful application of surface coating depends on two factors: the cohesion between the coating substance to be applied and the adhesion between the substrate and the film. The selection of the coating to be applied is purely based on the end application to be performed by the component. Till date many different plasma spray techniques like High Velocity Oxy Fuel (HVOF), Chemical Vapour Deposition (CVD), High Velocity Air Fuel (HVAF), and other techniques such as Laser Cladding, Shielded Metal Arc Welding (SMAW), etc. have been evolved and used for coating the substrate.

Thermal spray technique is widely used because it is very cost effective, but it does not produce metallurgically bonded coatings. The strength of coating layer is also low due to which it cannot bear high loads. There are various hard spots left in a coating layer which leads to high abrasion. PVD and CVD processes operate at high vacuums and temperatures which requires skilled operators. Moreover, they have very high capital cost, making the process very expensive. The rate at which coating is deposited is usually quite slow in addition to this appropriate cooling systems is also required as the process involves a large amount of heat. Nevertheless, laser cladding has potential to be one of the most promising surfacing technique widely being used in the anti-wear industrial applications [3-5]. The limitations of laser cladding are high initial setup cost, safety issues, lower deposition rates, high power requirements. Further, the laser is an intense heat source, which might cause confined thermal distortion and induced residual and thermal stresses on the substrate during cladding [6].

1.4 Factors of efficient material processing

The primary concern for the industries, research scholars and technologists is the effective and efficient processing of materials. As the energy requirements are increasing at an alarming rate, there is need to come up with more cleaner, sustainable and green technologies. Some of the major factors of efficient material processing are shown in Figure 1.4.

Figure 1.4: Various factors of efficient material processing

All these factors unitedly contribute towards a process which is effective, efficient and sustainable at the same time. If these factors are given utmost attention while developing a new manufacturing process, then all the limitations of conventional processes can be taken care of.

Recently, microwave processing of materials has appeared as a novel surfacing technique for developing cladding on metallic surfaces [7-11]. Microwave cladding covers almost all the limitations of the conventional surface processing techniques. It leads to uniform bulk heating which reduces the residual stresses, thermal gradient and thermal distortion on the target material and it also helps to attain metallurgically bonded surface layer without any cracks. So, this novel technique has promising future as it has many advantages over the other surface coating techniques.

1.5 Microwaves

Microwaves are a form of energy in the electromagnetic (EM) spectrum. These EM waves have a frequency range from around 300 MHz to 300 GHz. The credit of invention of modern microwave oven goes to American engineer Percy Spencer. In 1945, he accidently discovered the heating ability of microwaves while working for a company, developing microwave radar transmitters during World War II.

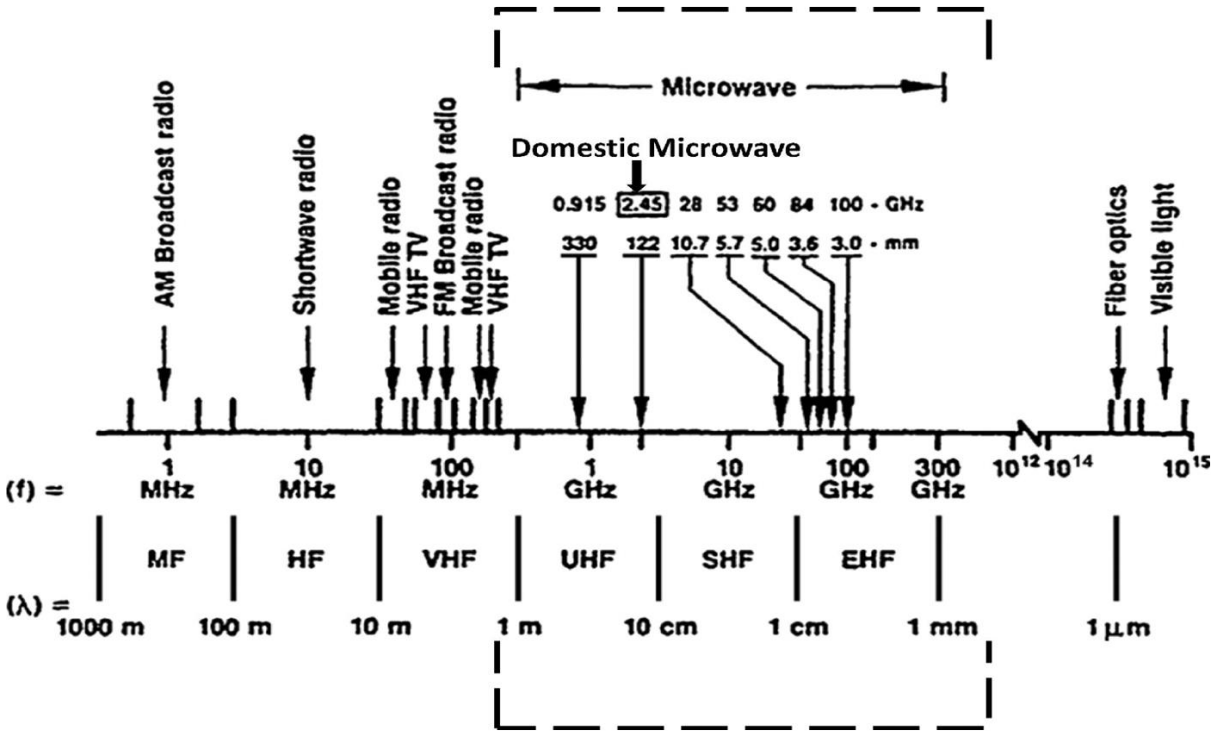

Figure 1.5: Wavelength and the frequency spectrum of electromagnetic radiations [12].

The microwave spectrum has a various frequency range which is used to serve numerous industrial and domestic applications. The domestic microwave ovens in most of the countries work at 2.45 GHz frequency. The application of microwave energy was carried in the field of material processing by the researchers.

1.5.1 Different application fields of microwave energy

In 1940, microwave technology was invented by two young scientists in England, they made an improved cavity magnetron tube which was used in World War II in radar systems. In 1946, an engineer named Percy Spencer while working for a magnetron manufacturing company accidently found the heating effect of microwave beam. Shortly after this incident, a

commercial microwave oven was developed for cooking purpose. Till 1965, applications of microwave energy were only limited to food processing, industrial heating and drying applications, rubber curing, etc [13].

Year by year more research was done in this area and researchers came up with a new approach of processing of ceramics through microwave heating [14]. Most of the work has been carried out in the field of sintering of several ceramics due to the fact that they tend to absorb microwaves at room temperature. In 2000, metallic materials were also in progress to be processed using microwave irradiations. Sintering of ceramics and metallic materials was followed by other processes like microwave cladding, microwave joining, microwave casting etc. The historical development in the field of the microwave is shown in figure 1.6.

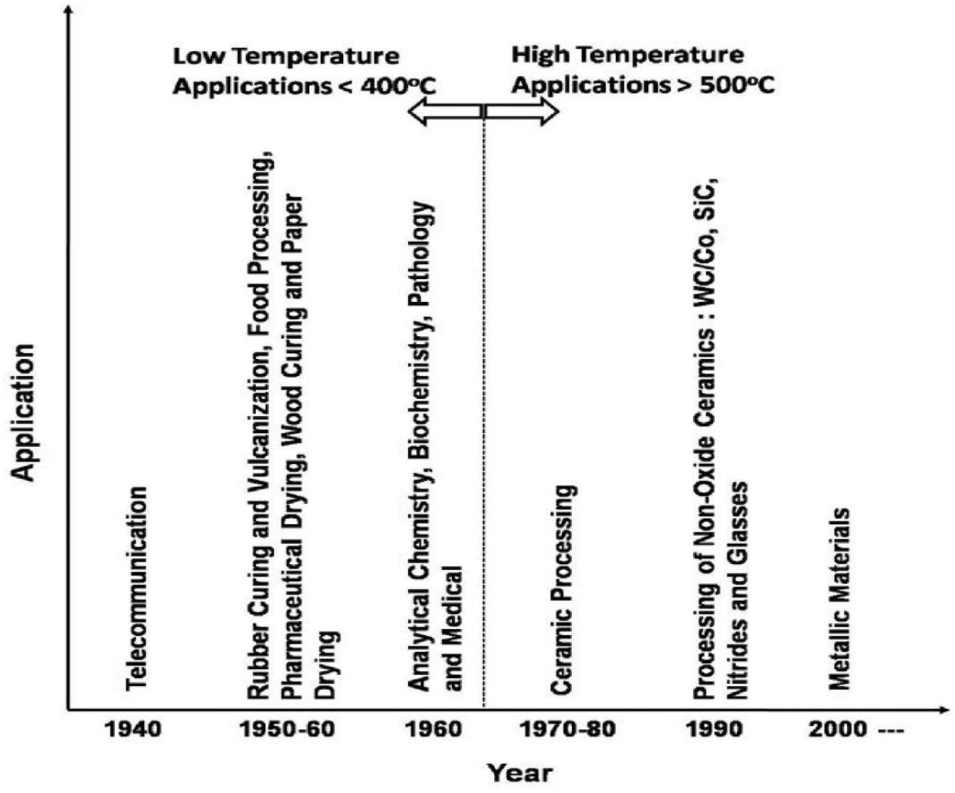

Figure 1.6: Chronological development in microwave processing [15]

1.5.2 Benefits of microwaves

Microwaves transfer heat to the material at a molecular level which helps to achieve uniform bulk heating ultimately reducing the thermal gradient and residual stresses on the target material. Moreover, microwave processing is a source of clean transfer of energy to the product being heated with increased energy efficiency using up to only 30% of the energy used by a conventional energy system. Research also reveals that microwave processing is not merely an

environment-friendly manufacturing technology, but it is also a sustainable manufacturing technology which works at higher rates at a lesser cost with shorter exposure time. Microwave processing systems are very compact also when compared with the conventional ones. It provide us with an improved product quality with the addition of selective energy absorption feature. Some of the major benefits of microwaves are shown in figure 1.7.

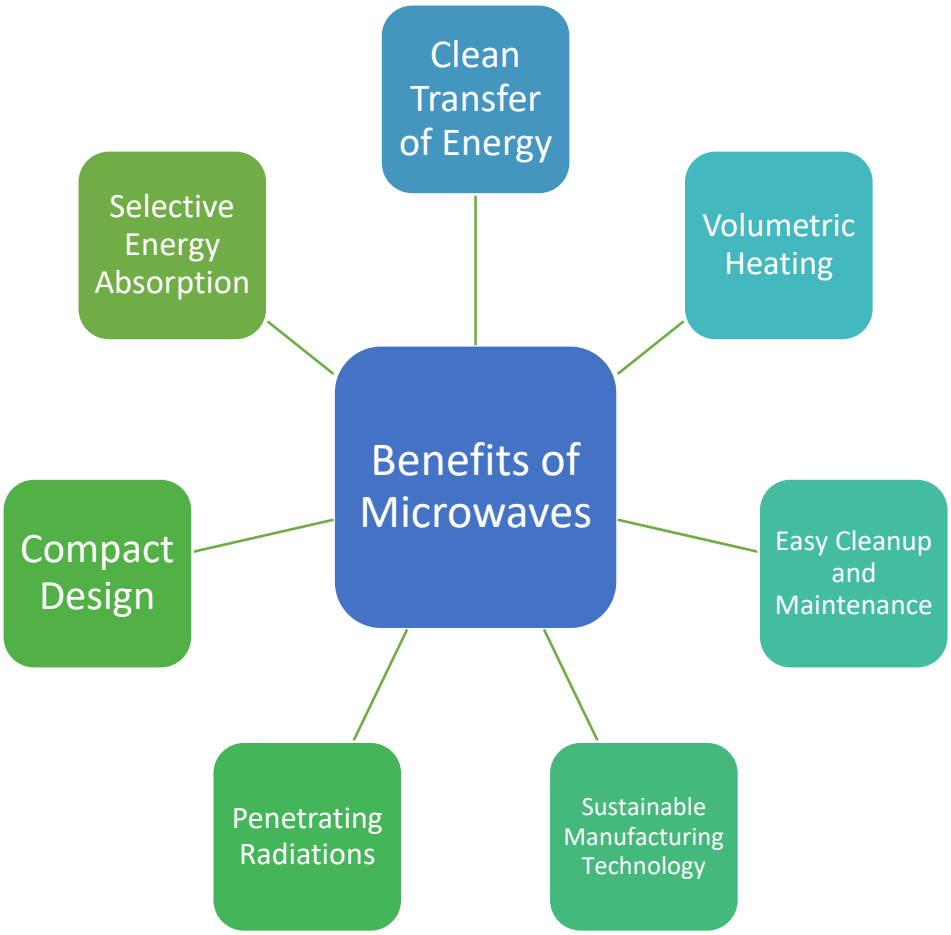

Figure 1.7: Various benefits of microwaves

1.5.3 Microwave Heating

Microwave heating is linked with the permanent dipole molecules motion initiated by the applied varying electromagnetic field. The permanent dipole molecules tend to re-orient themselves when they absorb microwave energy but their inability to react towards rapid reversals of the electric field leads to re-orientation losses. This re-orientation loss mechanism leads to power dissipation in the material because of phase lag.

Interaction of microwaves with the material is also an important aspect that should be known to a researcher. The physical properties of the material determine the interaction of the material

with the microwaves. If a material having a low dielectric loss tends to transmit the microwaves completely through them, then the materials are called transparent materials whereas the opaque materials tend to reflect back the microwaves due to high dielectric losses. Hence, heating of both the transparent and opaque material is not possible directly with the microwaves [16]. The materials which can directly absorb the microwaves are known as dielectric materials and they easily show volumetric heating in them. Figure 1.8 shows the interaction of different materials with the microwave radiations.

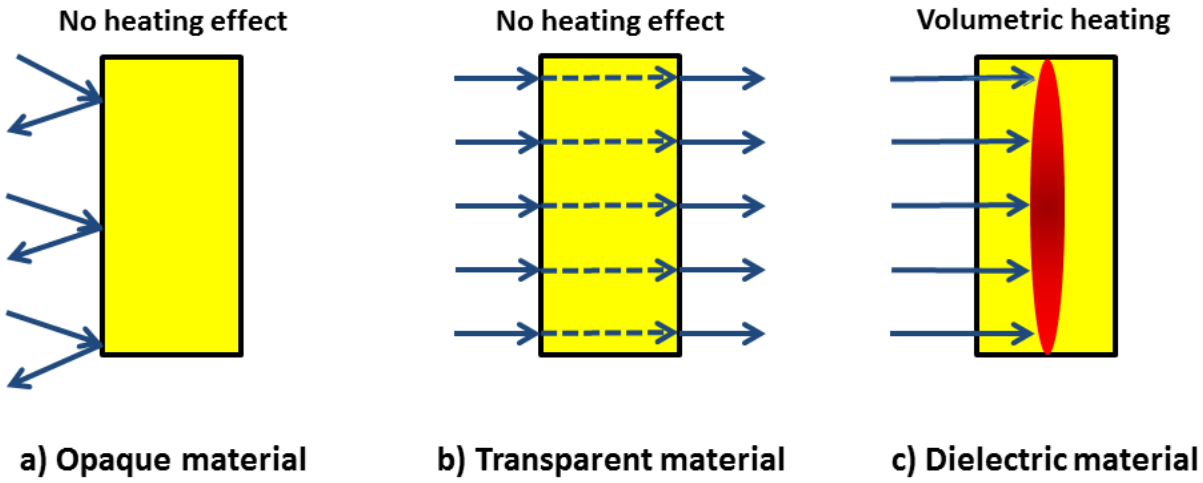

Figure 1.8: Different types of interaction of the material with microwave radiations

1.5.4 Difference between conventional and microwave heating

The heating phenomenon of conventional and microwave heating of material are very unlike. In conventional processing, the thermal energy is transferred starting from the surface to the core of the material with the help of conduction, convention and radiations whereas, in microwave processing, the electromagnetic energy is transformed into heat from within the material, which travels from the core of material towards the outer direction i.e. near the surface. This movement of heat from the core to the outer surface leads to the volumetric heating which eventually helps to rapidly heat the material, giving rise to reduced processing time, reduced thermal gradient and heat-affected zones, and lesser environment threats [17-18]. Figure 1.9 shows the direction in which the energy travels in the material during different modes of heating.

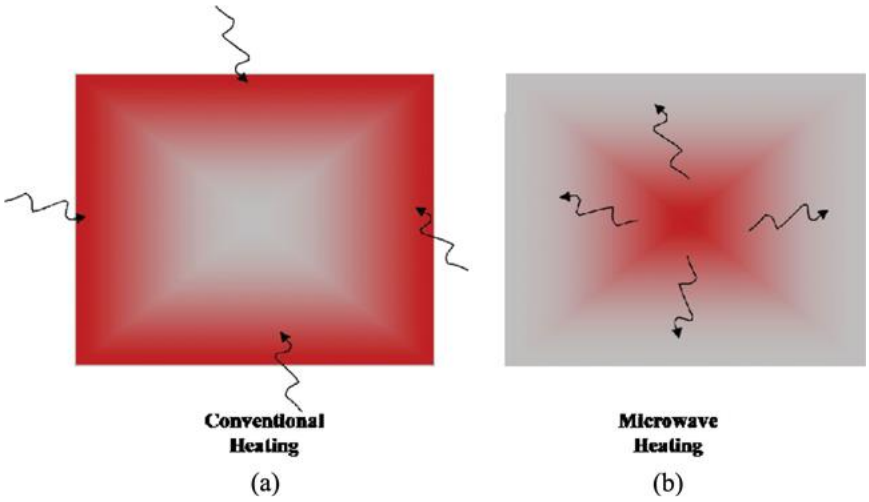

Figure 1.9: Different modes of heating (a) conventional heating (b) microwave heating

1.5.5 Microwave Hybrid Heating (MHH)

Microwave hybrid heating (MHH) is a technique of indirect heating which is used to overcome the problems in heating the material with low skin depth (low microwave absorbing material) [19]. The skin depth of materials is depth from the surface at which the incoming microwave power drops to 36.8% of the power value at the surface. The MHH technique uses two additional material known as susceptor and separator during the microwave processing to elevate the temperature of the material with low microwave absorbing capacity. Susceptor has the ability to couple with microwaves at room temperature and it gets heated up instantly. This developed heat is passed to the metallic powder through the separator, which is a transparent material and passes the microwaves without absorbing it, via a conventional mode of heating. When the metallic powder reaches its optimum temperature to start absorbing the microwaves directly, it will be heated through both conventional and microwave energy to attain the higher temperature. This process is known as MHH which leads to bi-directional heating of materials as heat is transferred from surface to the core through the conventional mode of heating and from core to the surface of material through microwave heating [20]. Figure 1.10 shows the process of MHH.

Separator while being the non-absorbing material also serves the purpose of separating the susceptor from the material under processing and it also allows the flow of heat from susceptor to the material through conduction. Graphite sheet or alumina sheet are frequently used separator material because they both have a low dielectric loss. Thus, the microwaves can easily pass through them without any interaction.

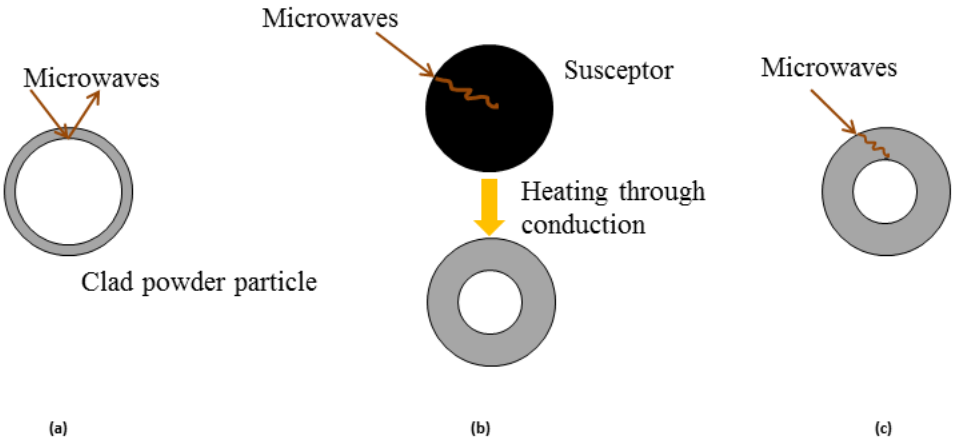

Figure 1.10: (a) Reflection of microwaves by clad material due to the small skin depth. (b) Addition of susceptor to increase the temperature of powder which in turn increases the skin depth of the clad material. (c) Absorption of microwaves directly by the clad powder

2.1 Literature Review

This chapter features the review of the literature based on the development of material processing through microwave energy. The literature consists of breakthrough developments in the field of material processing and research in the field of microwave sintering, joining, casting and cladding have been reported and systematically discussed in this chapter.

Aggarwal et al. (1999) [21] investigated on sintering of WC/Co based hard metals with the help of microwave radiation at 2.45 GHz frequency in a multimode cavity. A comparison on conventional sintering and microwave sintering was also done on the basis of ease of process, densification, physical, magnetic and mechanical properties. The author reported the achievement of full densification at a lower sintering temperature in company with lesser porosity whereas conventional sintering of WC/Co required high temperature. To achieve the higher temperature in conventional sintering, the lengthy thermal cycle of 10 to 14 hours are required which lead to WC grain growth and this increase in grain growth diminishes the mechanical properties of the metal being processed. It was observed that sintering and debonding happened in a single step, which resulted in improved physical and mechanical properties, in case of microwave sintering.

Cheng et al. (2002) [22] prepared transparent alumina (Al_2O_3) samples by microwave sintering process in single mode microwave system operating at 2.45 GHz frequency and 1.5 kW of power for small samples, and large samples were developed in multimode microwave applicator working at 6kW power. The grain growth and densification of alumina samples showed a lot of improvement because of a decrease in the energy required activation for sintering process. The microwave sintering of alumina samples was done at lower sintering time and needed lower sintering temperature in comparison to the conventional sintering technique. The author also reported the significant increase in conversion rate of polycrystalline alumina to single crystalline (sapphire) leading to improvement in transparency and other important properties of the alumina samples. The sample which was microwave processed for just 15 min showed good transparency with full densification.

Agarwal (2010) [23] studied latest global developments in the field of materials processed using microwave energy. Many ceramic materials like Al_2O_3, ZrO_2, $PbZr_{0.52}Ti_{0.48}O_3$ (PZT),

$BaTiO_3$ (BT) and WC-Co based ceramic metal composites were reviewed in detail for microwave sintering. The author also stated various advantages of microwave energy when used to process the materials, like reduction in processing time and cost savings, improved mechanical properties with fine microstructures and eco-friendly working environment. The author also provided an outline of steelmaking process through microwave energy and stated that there was 50% lesser emission of Co_2 in comparison to conventional routes. Various microwave applications like tire recycling, oil shale were discussed and almost 100% used tire contents were converted into useful products whereas microwave energy was successfully applied to heat oil shale in order to produce gases which can be converted to petroleum products with high calorific value.

Srinath et al. (2011) [24] illustrated a new approach for linking of bulk copper using multimode microwave applicator working at 2.45 GHz and power level of 900 W. 99.5% pure copper powder was used as a sandwich layer between a copper plate and coin to be joint metallurgically. Figure 2.1 shows the representation of the setup used for joining of metallic copper using MHH. Charcoal was selected as susceptor material to aid the microwave hybrid heating and exposure time was set to 900 s. The temperature of the copper particles was increased initially by susceptor through conduction, once the copper particles reach a critical temperature, it will directly couple with microwave leading microwave hybrid heating of the joint. The attainment of uniform microstructure confirmed the presence of volumetric heating throughout the joint. Copper changed its atomic number from 311 to 111 during microwave heating. The Vickers microhardness of 78 ± 7 Hv was obtained in bulk copper joint. Metallurgical bonding in the joint resulted in significant increase in tensile strength with greater elongation. The metallic material joining with the help of microwave heating is a fast, advanced and eco-friendly method.

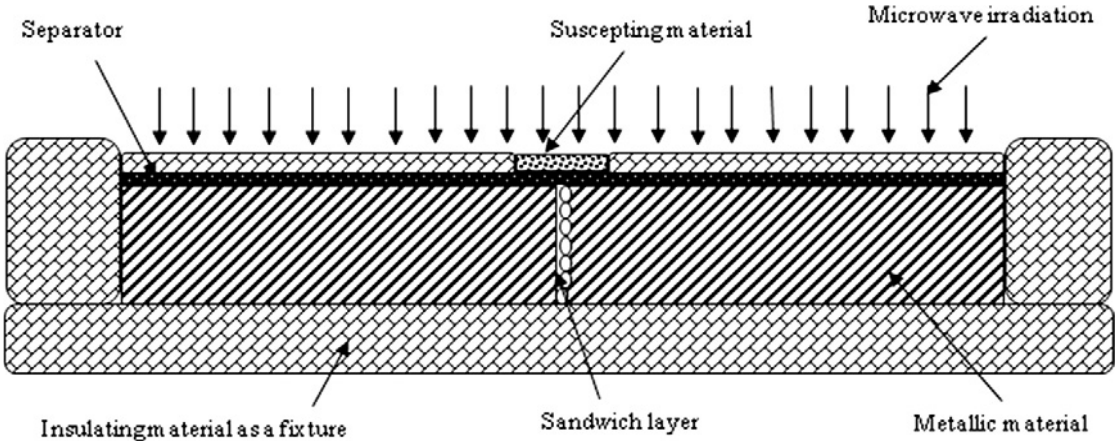

Figure 2.1: Representation of joining of metallic copper through of microwave hybrid heating process

Sexton et al. (2001) [25] investigated on a new repair technology using laser cladding for gas turbine components. Traditionally, tungsten inert gas (TIG) was used to repair the surface of gas turbine components but now, a new approach is used to clad the coating material onto aerospace component substrates which are known as laser cladding. The laser beam is directed over the substrate to form a melt pool, and powder delivery system is used to delivery powder on the melt pool along with carrier gas like air to avoid the occurrence of oxidation during the process. Figure 2.2 shows the schematic of laser cladding process. Laser cladding helps in diffusing the layer of fine alloy powder on the substrate without any pores and cracks. The developed clads showed good fusion bonding and minimal dilution as compared to the TIG clad samples. Low or narrow dilution zone in laser cladding samples gave rise to abnormal changes in hardness values from clad to the substrate, whereas the change in hardness in TIG clad samples were gradual and non-uniform due to the presence of wider dilution zone.

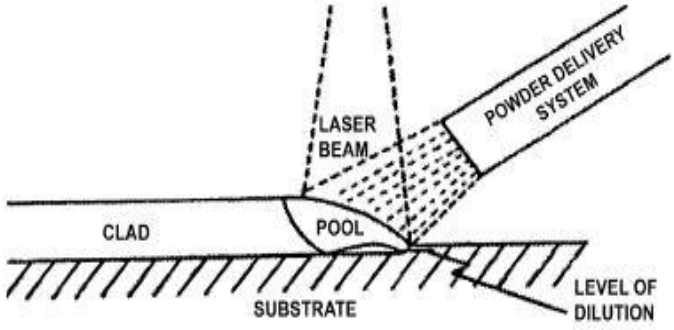

Figure2.2: Laser cladding process

Lo et al. (2002) [26] worked on the improvement of cavitation erosion resistance by laser cladding on the AISI 316 stainless steel surface using fine WC powder. A high power laser was used to deposit the powder layer on the surface of the substrate. A cavitation erosion testing machine was used to study cavitation erosion resistance of the developed samples, and substantial improvement in the cavitation erosion resistance was found, which was 30 times more than the bare substrate. According to the author, this high cavitation erosion resistance was due to the formation of carbide dendrites and interdendrites in the microstructure attained from the SEM images as shown in figure 2.3. The microhardness of the coated surface increased with the increase in the total content of tungsten (W) particles and formation of carbides. The author also stated that coating with fine carbides in the microstructure is more resistant to one containing coarse carbides.

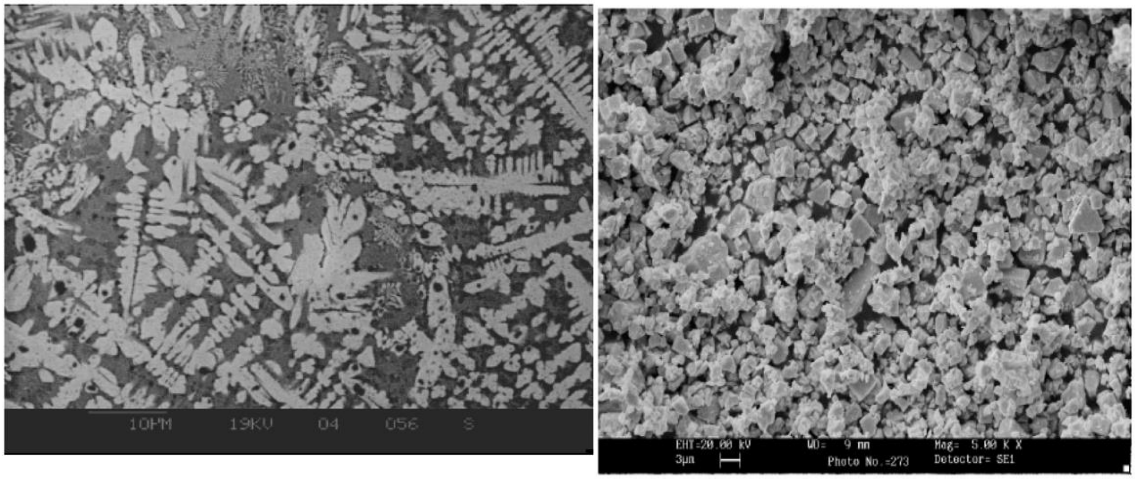

(a) (b)

Figure 2.3: SEM images of (a) laser surface-alloyed sample; (b) original WC powder

Liu et al. (2006) [27] investigated the laser cladding of Ni1015 alloy on a copper substrate using high power CO_2 laser. The specimen was freed from rust using solution of H_2SO_4 and HCl, and sandblasting of the surface of the specimen was done. Initially, the Ni-based powder was pre-deposited using plasma spray and later they were remelted using the laser with laser power set at 4 kW and scanning speed at 4 m/min. A metallurgical bonding was formed between the powder and copper substrate, as a large amount of Cu and Ni solid solution was present, which assisted in reducing the stresses, interfacial cracks, and pores on the coating. The microhardness of the developed clad was 280 Hv which was nearly 3 times that of the copper substrate.

Stella et al. (2005) [28] investigated on NiTi coatings sprayed using vacuum plasma spray on the surface of SS-316 L substrate. The developed coating samples were examined for cavitation erosion resistance using an ultrasonic cavitation testing machine as shown in figure 2.4. Two batches of coating were selected to be applied on the substrate, one was pre alloyed NiTi powder and the other was an elemental mixture of 50.8% Ni powder and 49.2% Ti powder. Cavitation erosion tests were carried on samples from both the batches and the results were compared. During the first 10 hours in a testing machine, both the coatings displayed mass losses because of elimination of low adherence particles in the pores. Pre alloyed powder coatings showed inferior cumulative mass loss than the elemental mixture coating which was due to the fine arrangement of non-shape memory phases.

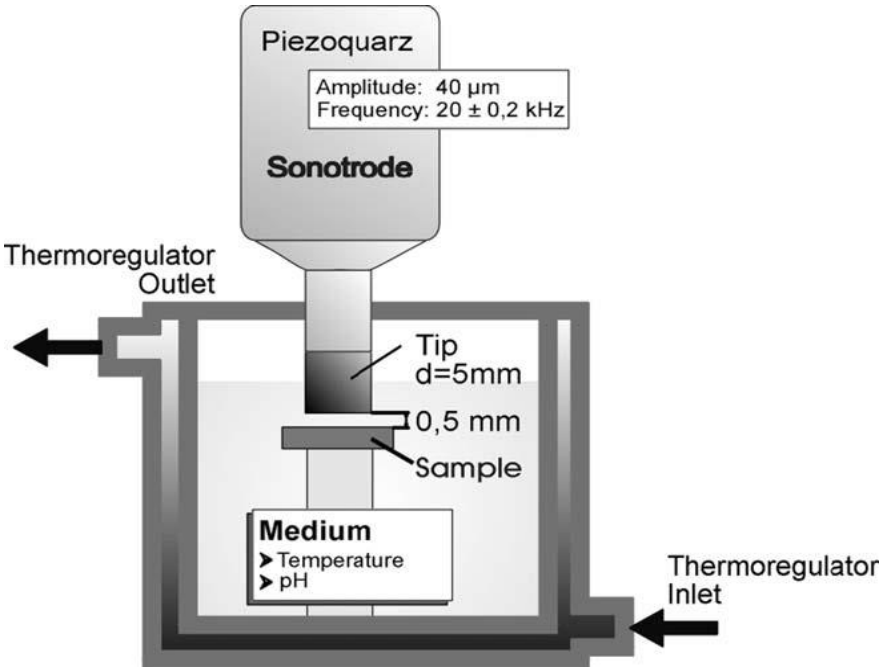

Figure 2.4: Sketch of the vibratory equipment used for testing cavitation erosion

Parco et al. (2006) [29] investigated on High Velocity Oxy-Fuel (HVOF) thermal spraying on two magnesium alloys which were AZ91 and AE42. WC-12Co was used as a coating material on the substrate. A high bond strength coating of WC-12Co spray powder was developed because of high kinetic energy associated with the spray powder leading to a self-roughening effect on the substrate. The WC-12Co powder as such didn't show any improvement in the corrosion resistance of the magnesium alloys but by applying an Al bond coating using duplex coating system, the corrosion resistance of the magnesium alloys can be increased significantly as shown in figure 2.5. The microstructure of the coating showed the formation of the very dense coating.

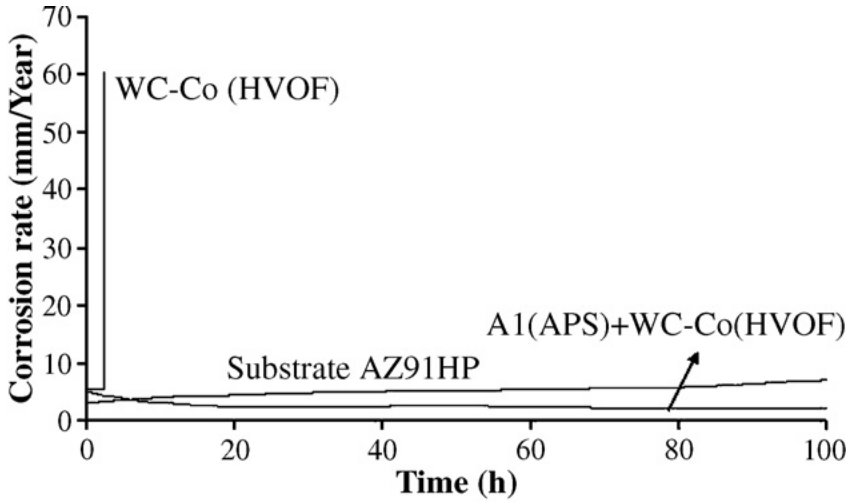

Figure 2.5: Corrosion rate in a 5% NaCl solution with constant pH

Gupta et al. (2011) [30] investigated a new surface processing method known as microwave cladding for improvement of surface properties of the SS-316 substrate. The author described the mechanism for developing microwave cladding using microwave hybrid heating (MHH) technique. The charcoal powder was used as a susceptor for absorbing the microwaves initially and transfers the energy to the powder through conventional routes. Once the powder reaches its optimum temperature, it will start to absorb the microwaves directly. This is known as MHH and the mechanism is shown in figure 2.6. Ni based powder was used as a coating material. The SEM image of clad confirmed that the thickness of clad was approximately 1 mm, which was without any visible interfacial and solidification cracks. The microstructure of the clad was found to be cellular in nature and had considerably less porosity. The microhardness of the clad was tested on Vickers microhardness tester and value of average microhardness was 304±48 Hv.

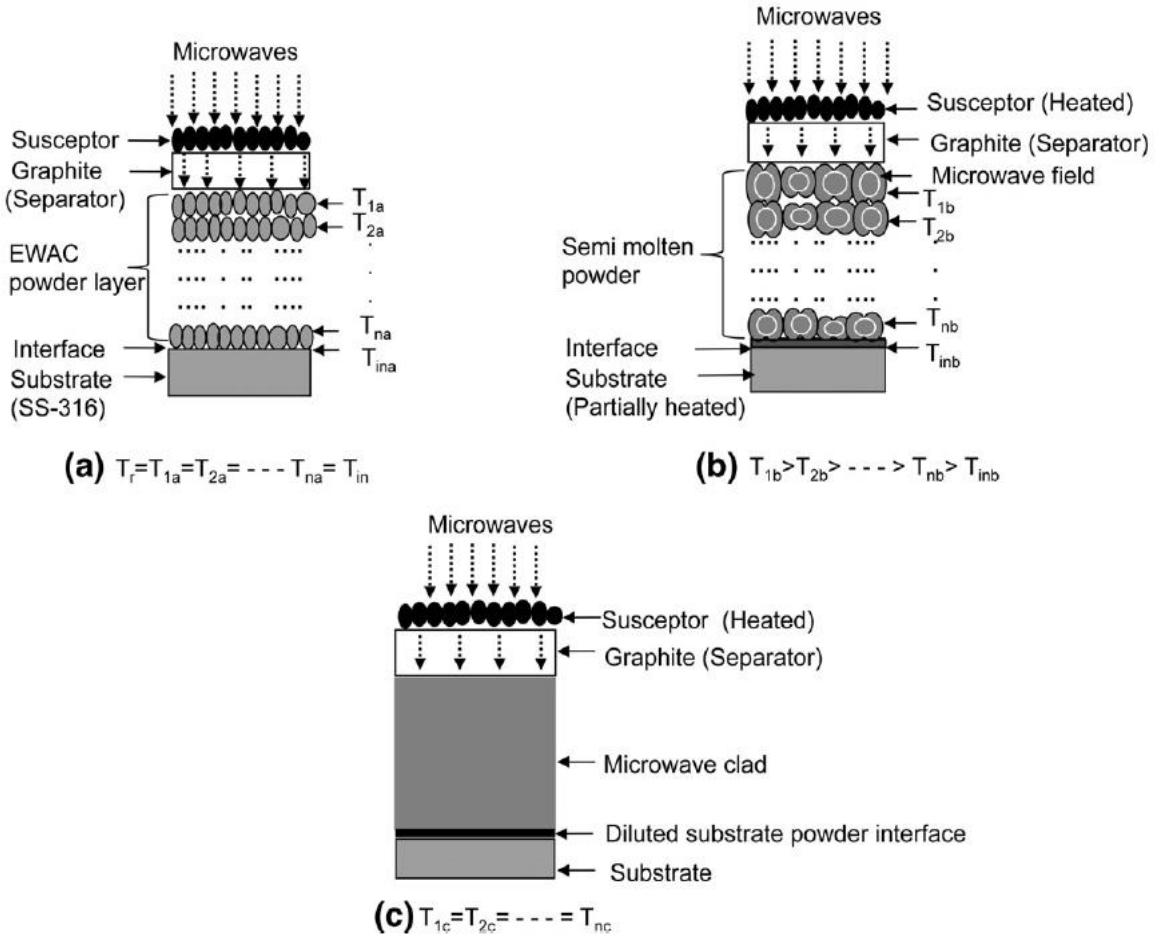

Figure 2.6: Mechanism of microwave coating- (a) initial condition, (b) powder starting to melt after absorption of microwaves, (c) formation of clad

Gupta et al. (2014) [31] developed a new approach in surface engineering in the form of microwave cladding. Microwave cladding of tungsten carbide (WC) based WC10Co2Ni powder was developed on SS-316 substrate having a dimension of 35 mm × 12 mm × 1 mm through microwave hybrid technique at 2.45 GHz frequency and power level of 900 W in a domestic multimode microwave applicator. Figure 2.7 shows the MHH set up used for developing clads. Characterization of the clads showed good metallurgical bonding without any cracks on the interface. Different elemental phases were detected by the XRD patterns of the clad region, showing the presence of carbides which was uniformly distributed all over the clad leading to increase in microhardness of the clad. The average Vickers microhardness of 1042 ± 124 Hv was observed in the developed clads which was very high compared to the microhardness of the substrate.

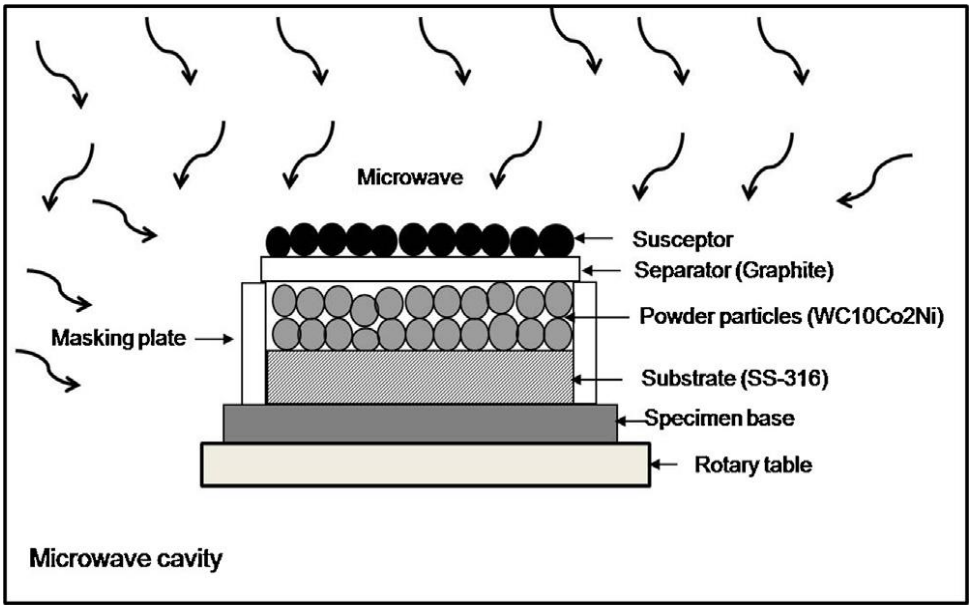

Figure 2.7: Demonstration of the MHH arrangement used for developing clad.

Zafar et al. (2014) [32] developed and characterized a WC-12Co microwave cladding on AISI 304 SS substrate. The clads were developed in an industrial multimode microwave system working at 2.45 GHz frequency and 1.4 kW of power. The clads were processed in the microwave for 600 s. Figure 2.8 represents the experimental setup used for developing microwave cladding. The developed clads showed good metallurgical bonding with the fractional melting of the substrate interface layer. The clads were uniformly heated owing to the Microwave Hybrid Heating (MHH) leading to crack free interface with less than 1% average porosity. The average microhardness of 1135±88 HV was witnessed which was 3.5 times more as compared to SS 304 substrate. Thus, the clads can be easily used in wear resistant applications. The various phases in the clad were detected with the help of XRD. Approximately

1 mm thickness of the clad was obtained over the substrate and uniformly distributed skeleton-like structure of hard metallic carbides was also seen in the magnified secondary electron image.

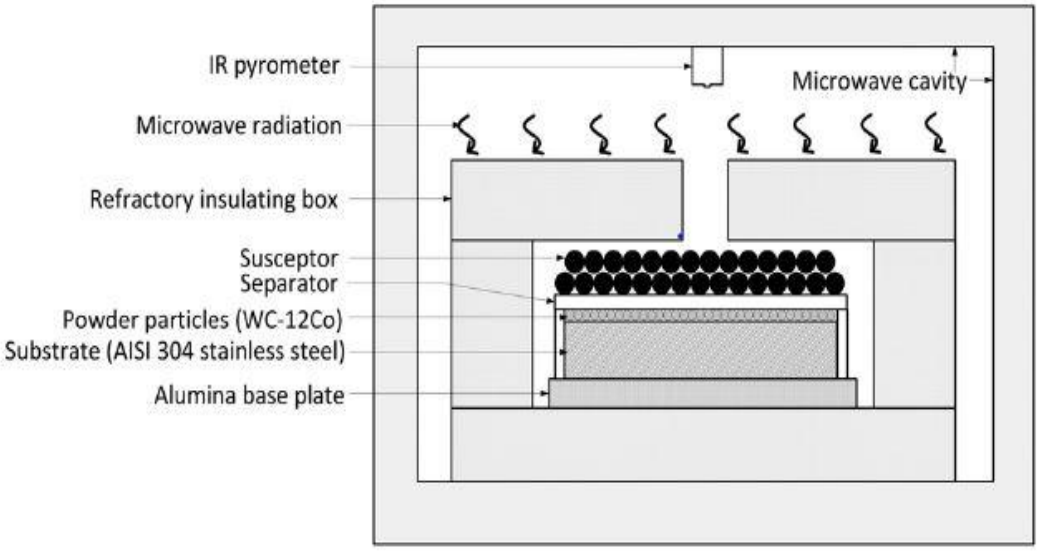

Figure 2.8: Graphics of arrangement used to develop microwave cladding.

Zafar et al. (2016) [33] investigated on flexural strength and residual stresses in micrometric and nanometric clads developed using MHH technique. The clads of WC-12Co were made in industrial microwave applicator and SS-304 was selected as the substrate material. The nanometric powder consists of the larger surface area than the micrometric powder, which gives the advantage of less exposure time and power needed to develop the nanometric clads because microwave interaction is quicker in them. Three-point bend test was used to assess the flexural strength of developed clads. The average flexural strength of nanometric clads was 14% higher than the micrometric clads because nanometric clads displayed more ductile deformation while flexural loading. Figure 2.9 represents the fractured samples after flexural strength test. Both nanometric and micrometric clads exhibited residual compressive stresses but nanometric clads showed 68% more residual stresses than the micrometric clads. The author concluded that the flexural strength of the developed cladding increases with increase in the magnitude of the residual stresses in the clad layer.

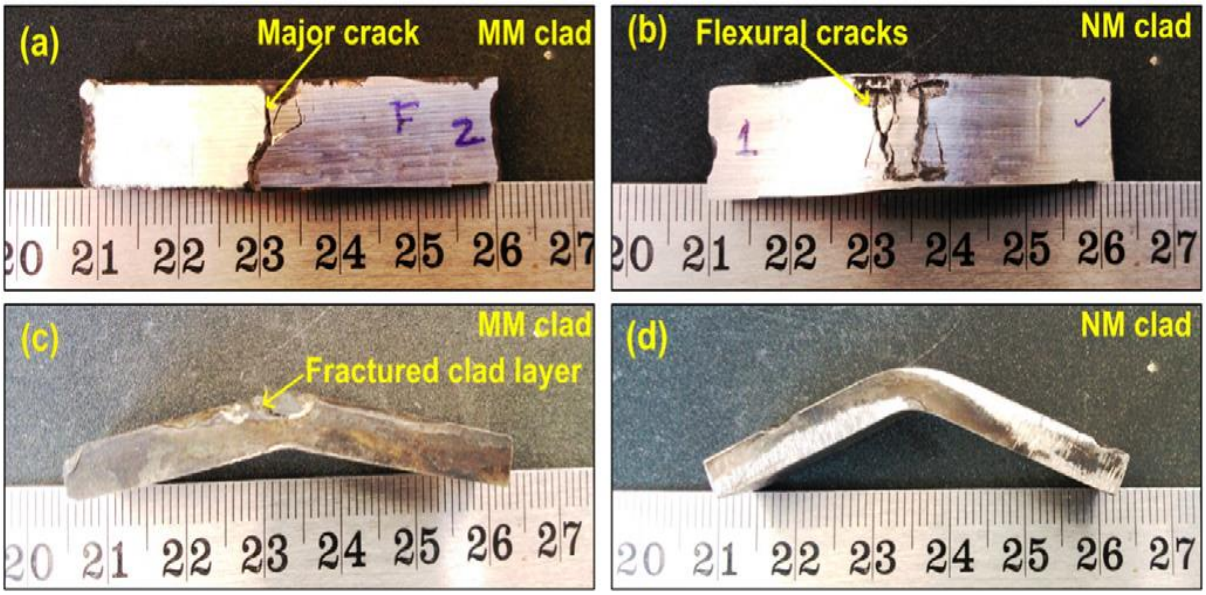

Figure 2.9: Picture of specimens after flexural strength test (a) top view of MM clad, (b) top view of NM clad, (c) side view of MM clad, and (d) side view of NM clad.

Singh et al. (2016) [34] examined a new approach of composite casting process through microwave hybrid heating. The castings of Ni+10%SiC powder mixture were successfully cast in the domestic microwave at 2.45 GHz frequency and exposure time was set to 18 min. The charcoal powder was used as a susceptor to initially heat the powder using conventional routes till it reaches the critical temperature. Once the powder reaches the critical temperature, it will start to absorb the microwaves directly. The SEM images revealed nearly equiaxed grains due to volumetric heating, and uniformly distributed hard particles of SiC in the soft Ni matrix due to the existence of convention current connected with electromagnetic energy as shown in figure 2.10. Microwave hybrid heating technique helped to decrease the processing time, saving the electrical energy consumption and it is also eco-friendly to the environment. The uniformly distributed SiC hard particles resulted in a high value of Vickers microhardness i.e. 1085 ± 210 Hv of the developed composite castings. Due to their high microhardness, developed castings can easily be used in anti-wear applications.

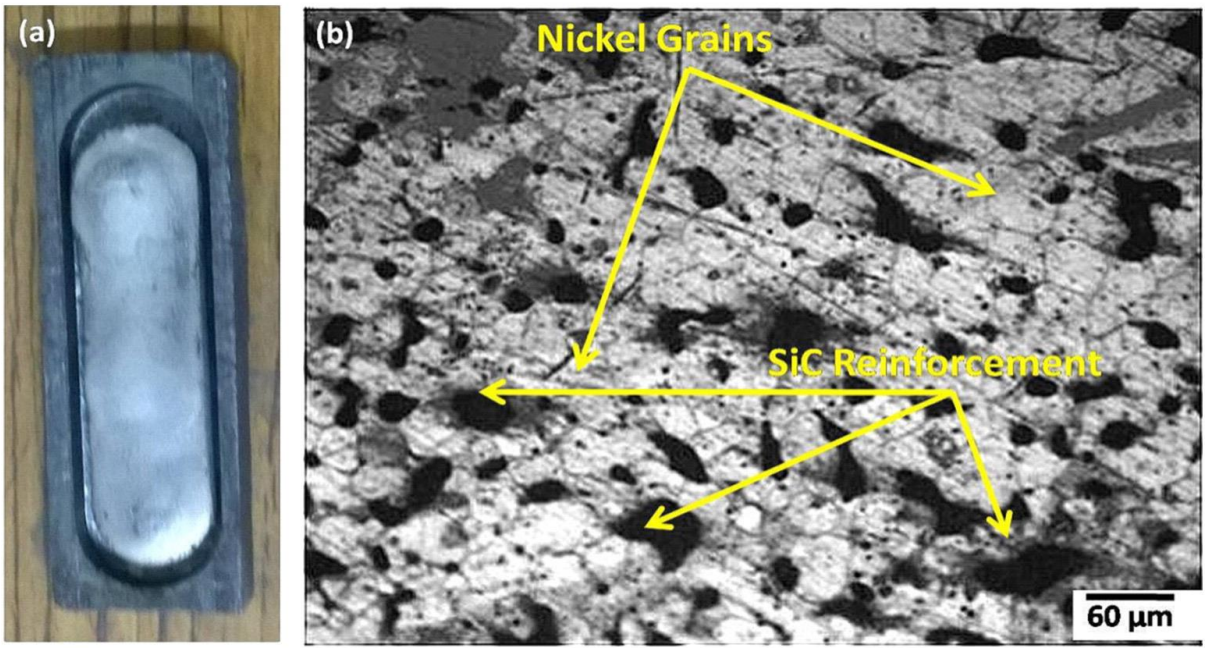

Figure 2.10: (a) Composite castings processed through microwave made of EWAC + 10% SiC and (b) image showing a scattering of reinforcement in the matrix phase.

Kaushal et al. (2017) [35] examined the microstructure and wear performance of the clads processed through microwave irradiation. Microwave cladding of Ni + 20% WC8Co was developed using domestic multimode microwave oven working at 2.45 GHz frequency and 900 W, on SS-304 substrate with the exposure time set to 300 s. MHH technique was used to develop the cladding. Dry sliding wear test of developed clads and SS-304 samples was carried out on pin-on-disc Tribometer with varying the parameters like sliding velocity, sliding distance, and normal load. It was found that the weight loss of the developed clads was significantly less than the SS-304 substrate. The SEM images showed uniformly distributed carbide particles inside soft Ni matrix without any microcracks and pores as shown in figure 2.11. The average microhardness was recorded to be 4 times higher than the substrate which was due to the uniformly distributed reinforced carbides.

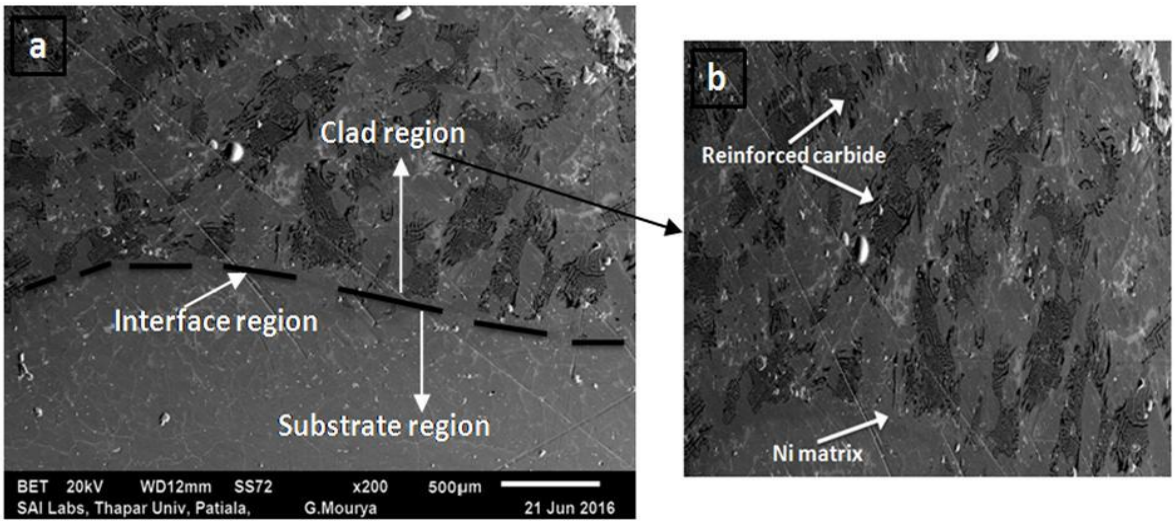

Figure 2.11: Image of clad showing (a) BSE image of the cross section of developed clad (b) zoomed view of the clad region

Lingappa et al. (2017) [36] examined a relative study on consumption of energy for melting of bulk non-ferrous metallic materials by conventional heating (muffle electric furnace) and microwave hybrid heating (MHH). Tin, zinc, aluminium, and brass were selected as the candidate materials for performing the comparative study. The candidate materials were melted in quantity of 50, 100 and 150 g and the corresponding time for melting the material was noted with their respective electrical energy consumption. The author concluded that the material processing time with MHH was significantly less than the conventional routes. The electrical energy consumption by microwave processing was also very less than the conventional heating process. Material processed by microwave energy exhibited a reduction in material wastage with the rise in the quantity being melted. The reason for less material wastage as stated by the author was the existence of bulk volumetric heating in microwave processed materials which eventually resulted in a reduction in thermal gradients.

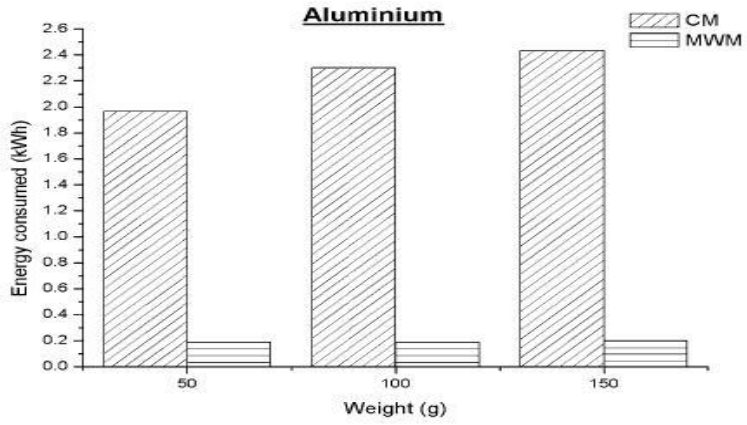

Figure 2.12: Comparison of energy consumption for MHH technique and conventional melting of aluminium

2.2 Summary of Given Literature

In the literature summarized above, a lot of work has been carried out in the field of material processing. The techniques like laser cladding, plasma spray, etc. were used widely for coating the substrate but microwave processing of materials has emerged as a novel technique. Many authors and researchers had worked on the process of microwave heating and they were successful in sintering, melting and joining of the metal powders. Different types of metal powders with varying compositions were investigated using microwave heating. Coating/cladding of metal ceramic powders on metallic substrates have been accomplished recently but still, there is scope left in the metal ceramic cladding by exploring the new compositions of metal powders to be cladded on the substrate to further enhance the mechanical, metallurgical and functional properties of the substrate using the MHH technique.

Chapter 3
Research Gaps and Problem formulation

This chapter demonstrates numerous literature gaps found in the existing literature. Based on these research gaps, formulation of the problem was done and work plan was also established to achieve the objectives.

3.1 Gaps in Literature

Thermal spray and laser cladding are the customary techniques preferred for surface modification of the substrate which comes with many disadvantages. To get rid of the limitations of these techniques, microwave energy is used to develop a protective coating on the substrate. In the early stages, microwave energy was widely used in the fields like telecommunications, food processing, chemical synthesis etc. With the passage of time, microwave technology was enhanced in terms of its heating capability and was used to process the ceramics, polymers, minerals and inorganic materials. Processing of metals using microwave irradiation is a challenging task because the microwave irradiation is not directly absorbed by the metals at the room temperature. So, the researchers came up with a new method which uses a medium, known as susceptor and separator, to couple metals with microwave energy and it is known as microwave hybrid heating (MHH) technique. The MHH technique has been mostly used for manufacturing processes like metal joining, sintering, casting and melting of metal powders. There is wide scope for research in the field of microwave cladding as only a little work has been noticed in this field. The claddings developed using microwave hybrid heating technique shows improved mechanical, microstructural and wear properties as compared to the coatings developed using conventional techniques. Some of the other gaps in literature are discussed below-

1. Improvement in clad Mechanical properties
2. Development of clads on complicated geometries
3. Reduction in clad porosity, solidification cracking, etc.
4. Improvement in Tribological behaviour

3.2 Problem Formulation

In the present scenario, the manufacturing companies want to come up with new cost effective and green manufacturing techniques so that they can survive in the age of cut throat competition. The primary objective of the present research is to develop a cost effective and

environment-friendly coating technique for developing wear resistant cladding through MHH by using a multimode domestic microwave oven. Processing of materials with microwave energy shows numerous advantages over the conventional modes of processing. Some of the major characteristics of the microwave heating are volumetric heating, selective energy absorption, easy clean-up and maintenance, green and sustainable manufacturing technology, etc.

The claddings developed through microwave radiations shows distinctive microstructure, enhanced mechanical and wear properties, takes lesser time to process the material than the conventional modes which reduces the manufacturing cost. However, processing of metallic materials through microwave energy is a thought-provoking task because the metallic materials do not absorb the microwaves directly at a common frequency of 2.45 GHz.

3.3 Objectives

The efforts of the present study will be to-

1. To Develop and investigate the wear resistant cladding through Microwave Hybrid Heating (MHH) by using multimode domestic microwave oven of 2.45 GHz frequency.
2. To study the effect of process parameters like exposure time, exposure power and preheating temperature of the powders.
3. Characterization of developed clad through Scanning Electron Microscope (SEM), Energy Dispersive X-ray Spectroscopy (EDS), X-ray Diffraction (XRD), Vicker's micro-hardness tester and Flexural strength.
4. To investigate the wear performance of cladding by using Pin-On-Disc Tribometer.

3.4 Work Plan

To achieve the objectives of the research, work is to be carried out in three phases:

Phase 1: Selection of substrate and cladding material

Phase 2: Development of cladding through microwave processing

Phase 3: Characterization of the developed cladding

The anticipated plan of the research work is shown in the flow chart below.

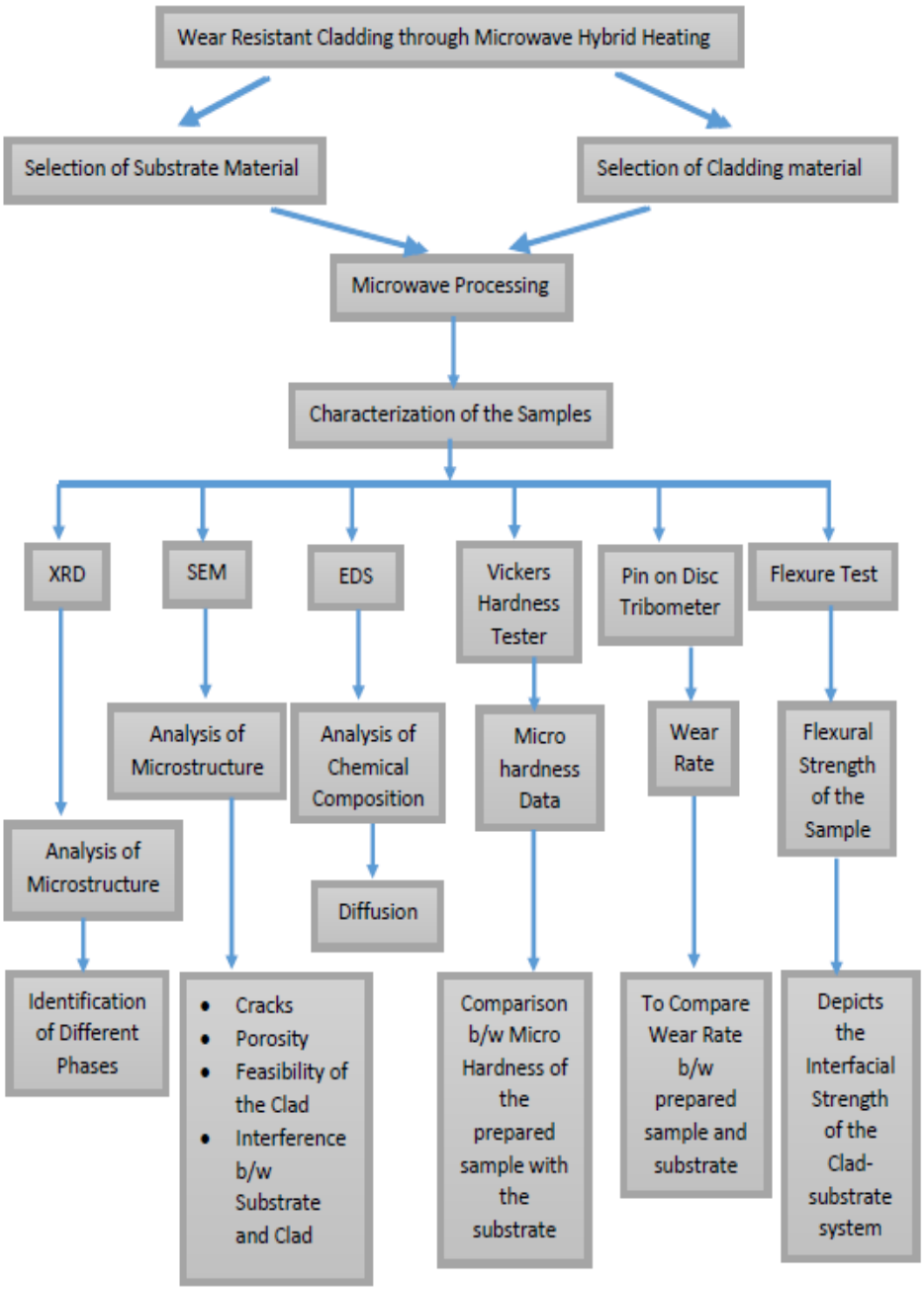

Figure 3.1: Flow chart of the work plan

Chapter 4
Material Selection

4.1 Introduction

The selection of material itself is a very challenging task. One has to select the material very wisely as it is the foundation step of the whole experiment. Selection of matrix material and reinforcement material to make a composite wear cladding is a very perplexing task as the metallic powder do not couple with microwaves directly and very limited work has been carried out in this field.

4.2 Selection of substrate

An Austenitic stainless steel (SS-316 L) has been selected as a substrate material. The austenitic stainless steel (SS-316 L) with 2.0 to 3% Mo provides good resistance to pitting corrosion but when used in gas turbine plant and hydro power plant, they are subjected to very severe working conditions leading to more frequent failures. In this case of severe wear applications, these steels undergo metallic wear due to the formation of adhesive junctions. The failure of these materials results in a huge economic loss to the growing countries like India. The solution to the above problem is either to replace the material component with a new one or to modify the surface of material component vulnerable to metallic wear. The replacement of the damaged component by a new one is not cost effective solution. Hence, surface modification of SS-316 L is one of the best and eminent solutions to this limitation.

4.3 Selection of matrix material

Nickel and nickel based alloys have been found to be resistive against wear and corrosion and they are commonly used in power generation, marine and aviation applications. They have properties of high strength, wear and corrosion resistance at elevated temperatures. The nickel based powder containing more than 97% Ni-based powder (EWAC 1004EN, Make: Larson & Toubro, India) is selected as a matrix material. EWAC powder has an average size of 40 µm.

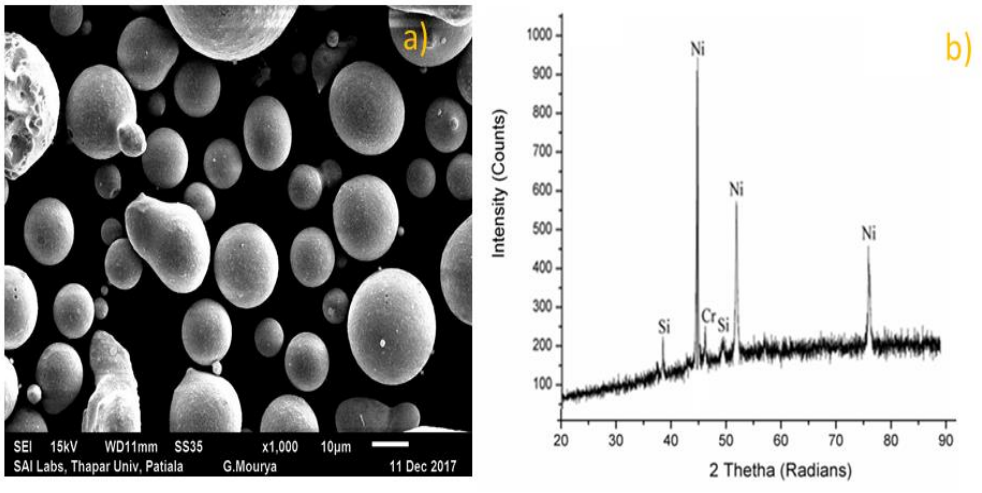

Figure 4.1: SEM image of raw matrix powder a) Ni based (EWAC) with corresponding XRD spectra of b) Ni based (EWAC) powder

4.4 Selection of reinforcement material

The function of reinforcement material is to provide better properties when added to the metal matrix. It is used to increase the hardness, toughness, and strength of the composite material. The selection of reinforcement material totally depends on the desired properties to be achieved by the researcher. The composition of reinforcement to be added is also an important parameter which is to be taken care of. In the present work, tungsten carbide powder (WC-8Co), molybdenum powder (Mo), chromium carbide powder (Cr_3C_2) were selected as the reinforcement materials to be added in a certain amount to the matrix to form the desired composite material.

Table 4.1: Chemical composition of matrix powder, reinforcement powders and SS-316 L

Material and powders	Elements									
	Fe	Cr	Ni	C	Mo	W	Si	Mn	Co	Others
SS-316 L	Bal.	17.3	11.1	0.02	2.2	0.04	0.2	1.3	0.2	0.5
Ni-based	-	0.17	Bal.	0.2	-	-	2.8	-	-	-
WC-8Co	-	-	-	14.19	-	72	-	-	7.32	6.49
Cr_3C_2	-	86.64	-	13.34	-	-	-	-	-	-
Mo	-	-	-	-	94.69	-	-	-	-	Bal.

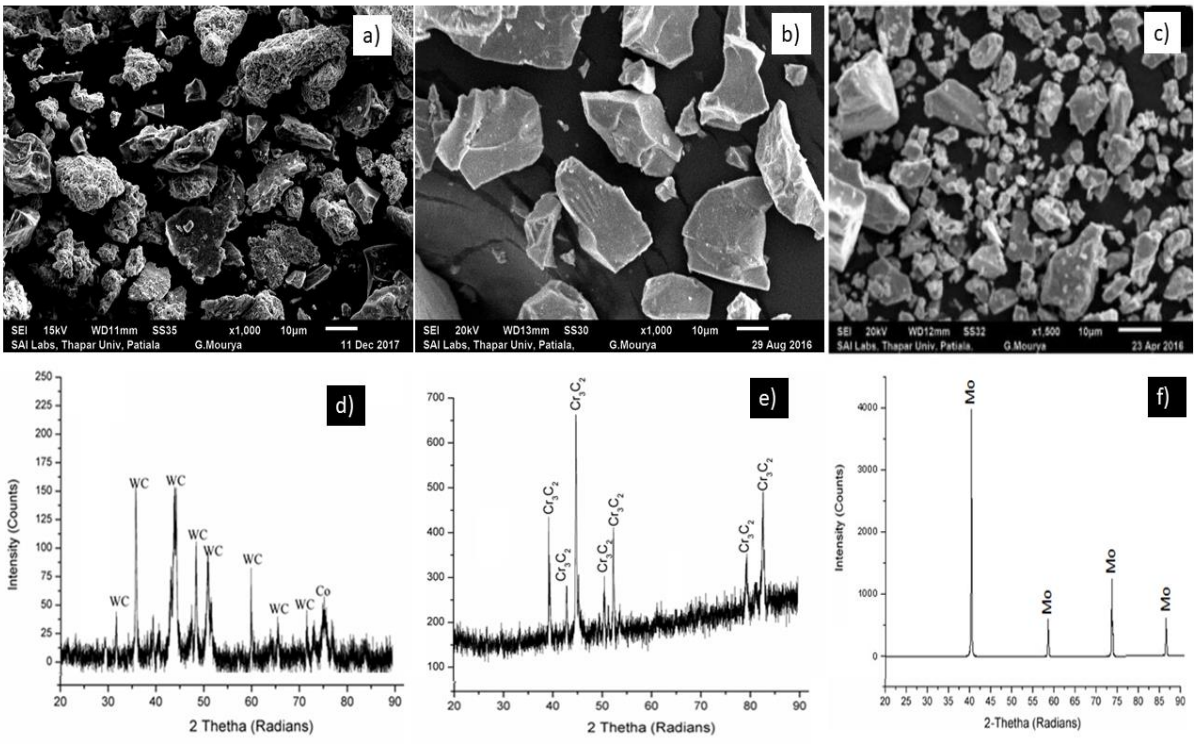

Figure 4.2: SEM images of raw reinforcement powder a) WC-8Co, b) Cr_3C_2, c) Mo with corresponding XRD spectra of d) WC-8Co powder, e) Cr_3C_2 powder, f) Mo powder

Chapter 5
Experimental Setup

5.1 Introduction

The development of a new method to process a variety of material requires well planned approach for experimentation so that we can easily achieve our objectives. The process parameters has to be optimized and the theory and science behind the process has to be clear and known. This section of the thesis will introduce you to the process of clad formation and different methods that were used to characterize the cladding.

5.2 Clad formation

Before starting with the clad formation, the compositions for the powder to be cladded were decided. Two different compositions were prepared as shown in the table-

Table 5.1: Compositions decided to develop microwave processed clads

S.NO	Description
1	70% Ni-based + 20% WC8Co + 10% Mo (Ni-based20WC8Co-10Mo)
2	80% Ni-based + 10% WC8Co + 10% Cr_3C_2 (Ni-based10WC8Co-10Cr3C2)

A domestic multimode microwave with 900 W of power and working at 2.45 GHz of frequency was used to develop the clad and 99% pure alumina sheet (Al_2O_3) (Make: Ant Ceramics Pvt. Ltd.) of 1mm thickness was used as a separator. Charcoal powder with 14% carbon was used as a susceptor.

As the skin depth of the powders to be cladded is very low as compared to the particle size of the powders itself, the mixture of these powder cannot absorb the microwave directly instead it tends to reflect them. In order to get rid of this problem, MHH technique using a suitable susceptor is employed. The temperature of the susceptor increases rapidly as it couples with the microwaves at room temperature easily, which in turn, increases the temperature of powder particles through separator via convection. Once the powder particles reach its optimum temperature, it will start to absorb the microwaves directly and start to get heated and melted. MHH gets its name from here only as it is a hybrid heating technique rather than using only microwaves, both the convection and microwaves are used to develop the cladding.

The substrate was cleaned with the help of emery papers of different grit sizes to get a uniform and shiny surface so that powder may stick easily with it. The mixture of powder to be deposited was preheated at 180^{o} C to remove any moisture if present. Then, the powder was manually placed on the substrate to get a uniform thickness of around 1 mm. After placing the powder, the substrate is placed on the refractory brick. Now, the separator is placed on the substrate carrying powder, to prevent any mixing or contamination of powder with charcoal powder placed above the separator. These were the steps to prepare the substrate for cladding. Now, the refractory brick is placed on the rotary table in the microwave and the time of exposure is set to 360 seconds.

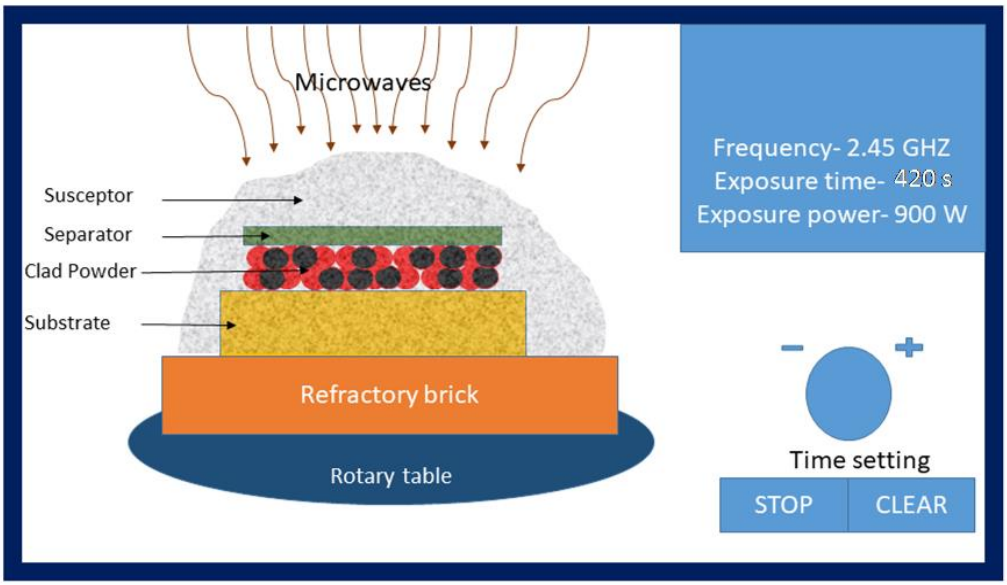

Figure 5.1: Schematic representation for developing clads using microwave hybrid heating technique

Table 5.2: Process parameters for development of microwave cladding

Parameters	Description
Applicator	Multimode (Model: Charcoal, Make: LG)
Frequency	2.45 GHz
Exposure time	180-420 s
Exposure power	900 W
Powder preheating temperature	200^{o}C
Powder	Ni-based20WC8Co-10Mo, Ni-based10WC8Co-10Cr3C2
Susceptor	Charcoal powder
Separator	99% pure alumina sheet (1 mm thick)

5.3 Characterization of cladding

5.3.1 Diamond cutter

A diamond cutter is a low speed saw unit (Model: MS-10, Make: Ducom Instruments Pvt. Ltd.) used to cut various hard materials using diamond wafering blades. The low speed of the tool is used to cut the clad specimen along the thickness to get the very high quality of cut and minimal deformation, without damaging the surface of specimen because the same specimen will be characterized through SEM. The specimen is gravity fed as they are small and delicate.

Figure 5.2: Diamond cutter

5.3.2 Polishing

After cutting the samples along the thickness, they were polished with the help of emery papers of grit size 150, 220, 320, 600, 800 respectively. The samples were polished to remove any type of contamination present on the surface of clad. The samples were then polished on a disc polisher which consists of two rotating wheels, first wheel was mounted with emery paper of fine grades starting from 1000 to 2000, 3000 and 4000 were used in series and second wheel was covered with soft velvet cloth over which diamond paste was spread evenly to get shining surface without any scratches so that microstructure of the sample can be seen easily during SEM.

Figure 5.3: Disc polisher

5.3.3 X-ray Diffraction (XRD)

XRD is a non-destructive analytical technique designed to give detailed information about crystalline compounds, including detection and quantification of crystalline phases. It is the simplest and most economical technique available at the time. The X-rays are generated through cathode ray tube and they are directed towards the sample. When the incident rays interact with the sample, diffracted rays are produced, satisfying the condition of Bragg's Law ($n\lambda = 2d \sin\theta$). These diffracted rays are then detected, processed and counted to get an XRD pattern. All the measurements were carried out at room temperature in the diffractometer using Cu $K\alpha$ radiations. The scan rate for XRD was set at 1° min^{-1} in the scan range of 15° to 90°. The machine is present in SAI Labs of Thapar Institute of Engineering & Technology.

Figure 5.4: X-ray Diffraction (XRD) machine

5.3.4 Scanning Electron Microscope (SEM) and Energy Dispersive Spectroscopy (EDS)

A SEM produces images of a sample by scanning the surface of the sample with help of focussed beam of electrons. It is a type of electron microscope in which the electrons interact with atoms to reveal information about the sample regarding surface topography, morphology and crystallographic information at very high magnifications. The SEM (Model: JEOL JSM-6510LV, Make: Oxford Instruments) is available at SAI Labs of Thapar Institute of Engineering & Technology.

The SEM equipped with EDS is useful in finding the chemical composition of the sample. It can estimate the relative concentrations on the surface of the sample down to a spot size of a few microns, and to develop element composition maps like area mapping and line mapping.

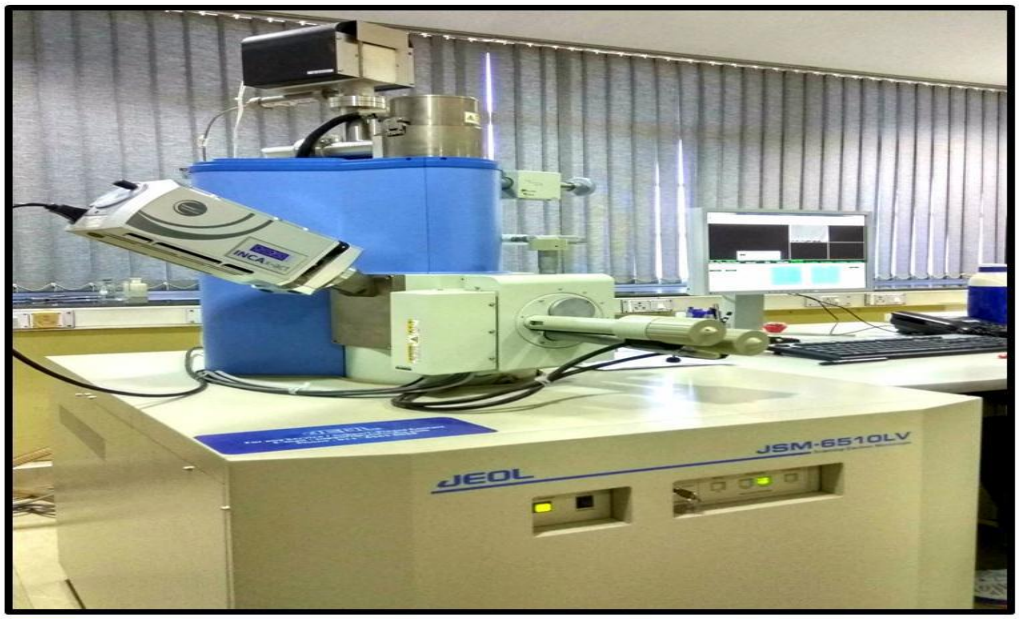

Figure 5.5: Scanning Electron Microscope (SEM)

5.3.5 Microhardness

The samples were cut along the thickness to evaluate their structural property correlations using Vickers hardness tester (Make: MetaTech; Load Range: 5g to 1Kg). The measurements were carried out at 300g load with a dwell period of 20 s.

Figure 5.6: Vickers microhardness tester

5.3.6 Wear test

The dry sliding wear test was performed on a pin-on-disc-Tribometer (Make: Ducom India; Model: TR20LE). The clad faces were employed as the wear pin, having dimensions of 8 mm x 8 mm x 6 mm, and alumina disc maintained at 76 HRC hardness was selected as the counter surface. The wear pins were held firmly inside the 8ϕ V groove pin holder. A Design of Experiment was prepared, selecting sliding velocity and load as the process factors. The weight loss was determined by keeping the sliding distance fixed at 2000 m for every sample at a rotational speed of 0.5, 1 and 1.5 m/s. The weight loss was measured after the interval of 500 m.

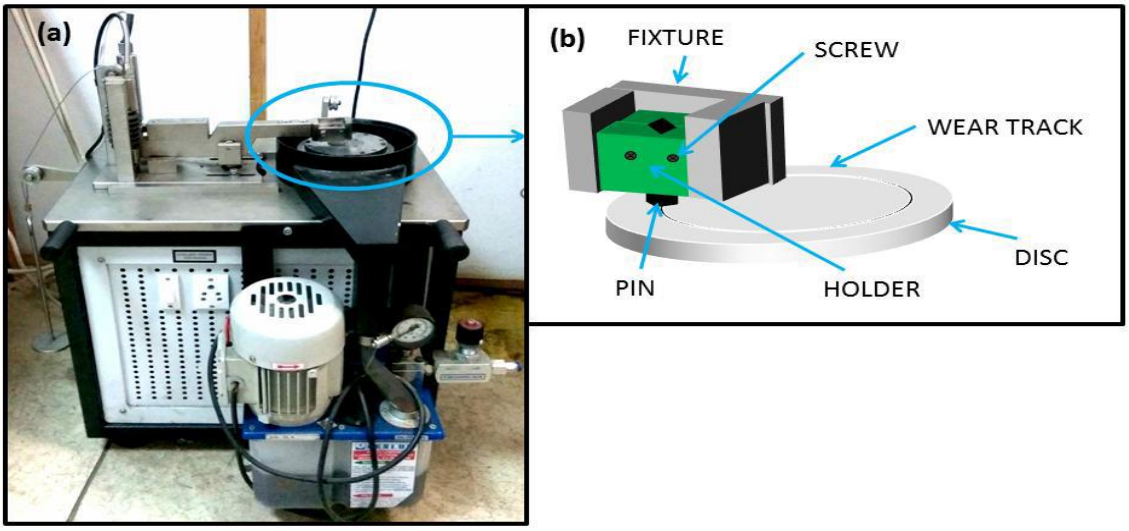

Figure 5.7: Pin on Disc Tribometer (a) Photograph and (b) Schematic representation of setup

Table 5.3: Process parameters for dry sliding wear test of developed clads and substrate

Parameters	**Description**
Test setup	Pin-On-Disc Tribometer
Wear Pin	a) SS-316 L b) Ni-based + 20% WC + 10% Mo c) Ni-based + 10% WC + 10% Cr_3C_2
Counter disc	Alumina plate, Hardness ~ 1400 HV
Sliding distances (m)	500, 1000, 1500 and 2000
Sliding velocities (m/s)	0.5, 1 and 1.5
Normal load (N)	10, 15 and 20
Lubrication condition	Dry
Temperature (°C)	Room temperature

5.3.7 Flexural test

The flexural performance of the developed clads is evaluated using Universal Testing Machine (UTM). A three-point bend test setup is employed on the machine to calculate the interfacial strength of the specimen. The flexural strength of the specimen significantly affect the structural, mechanical and wear performance of the claddings on metallic substrates. The size of the specimen to be tested was kept as 50 x 12 x 6 mm^3. The flexural strength of the specimen is calculated using following Eq.

$\sigma = 3\ FL / 2WT^2$

Where,

σ = bending strength

F = force at the fracture point

W = width of the specimen

T = thickness of the specimen

L = length of the support span

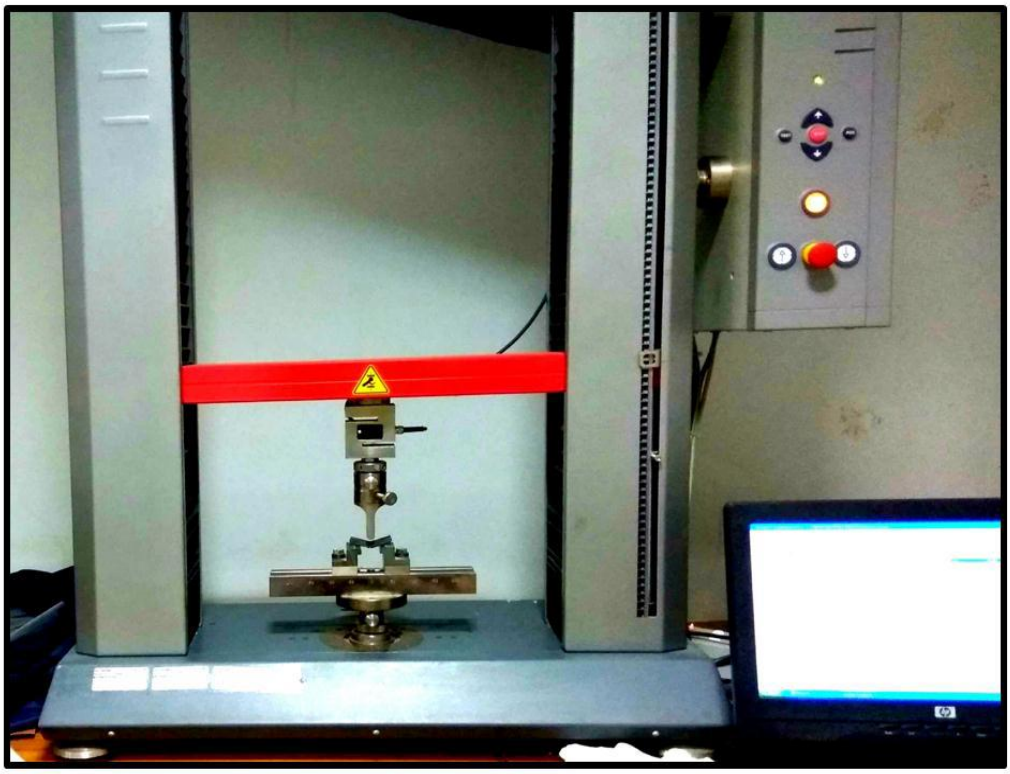

Figure 5.8: Universal Testing Machine (UTM)

6.1 Introduction

In the present study, composite clads of Ni-based10WC8Co-10Cr3C2 and Ni-based20WC8Co-10Mo have been successfully developed on SS-316 L substrate using a domestic multimode microwave oven working at 2.45 GHz frequency. The clads were developed using Microwave Hybrid Heating (MHH) technique at a power level of 900W. The following chapter describes the results of the characterization of the developed clads.

6.2 Microstructure Analysis

SEM and EDS analysis of the developed composite clads were carried out to compare the microstructure of the clads which are discussed in the following sections:

6.2.1 Microstructure Analysis of Ni-based10WC8Co-10Cr3C2 cladding

A microwave processed clad is characterized as good if it is free from defects like cracks and pores, provided it should have excellent metallurgical bonding with the base material. The BSE image shown in figure 6.1 is displaying the crack free wavy interface between the clad region and substrate. The presence of WC and Cr_3C_2 particles was confirmed from the expanded view of the clad region, which was arbitrarily dispersed in the Ni matrix. These dispersed WC and Cr_3C_2 particles deliver overall strength to the developed clad. The thickness of the developed clad was recorded to be 0.8 mm.

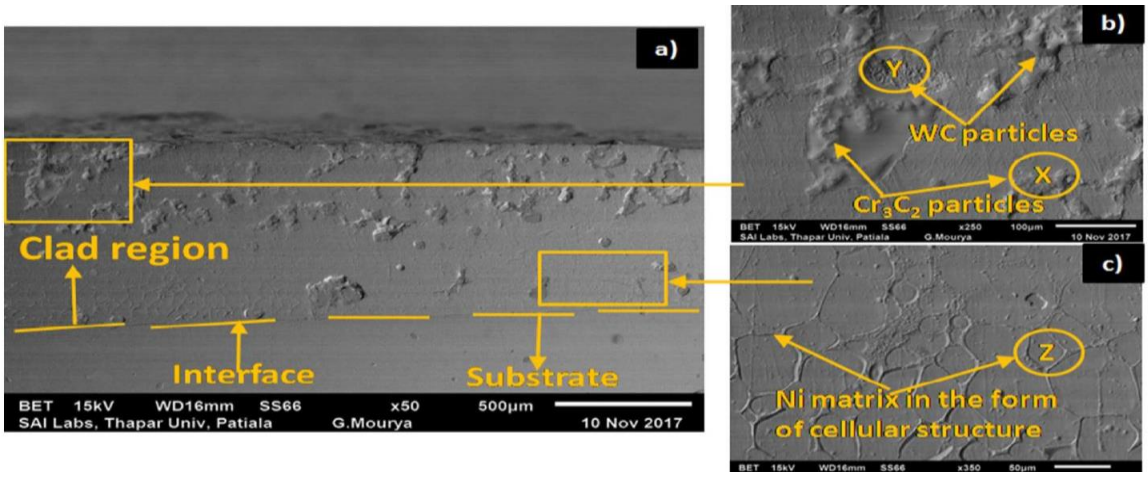

Figure 6.1: BSE image showing (a) cross section of clad (b) hard carbides region (c) soft Nickel matrix region

6.2.2 Elemental study of Ni-based10WC8Co-10Cr3C2 cladding

The EDS analysis of the BSE image of the clad region was also executed to verify the presence of different particles. The analysis verified the presence of reinforced Cr_3C_2 particles at point X, hard carbides of WC at point Y and soft Ni particles at point Z in agreement to the figure 6.2.

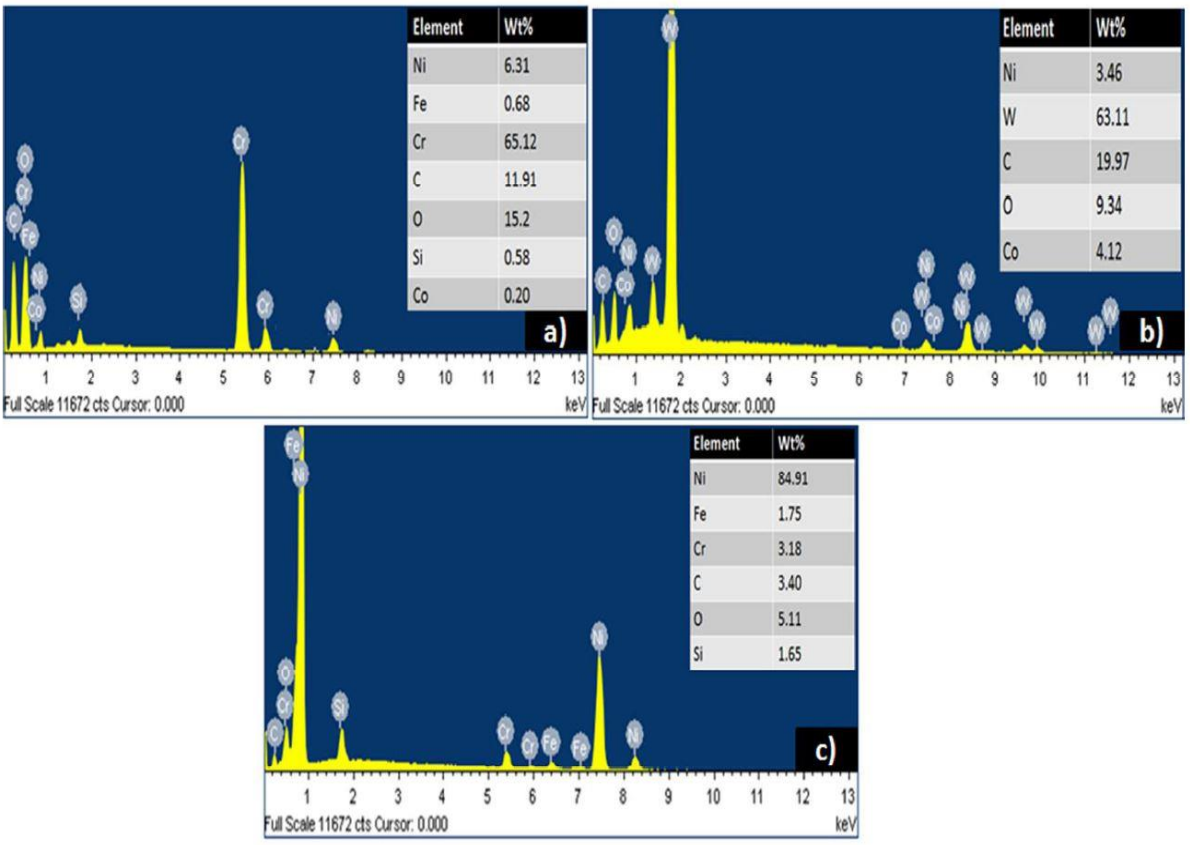

Figure 6.2: EDS analysis at (a) point X corresponding to figure 6.1 (b), (b) point Y corresponding to
figure 6.1 (b), and (c) point Z corresponding to figure 6.1 (c)

The area mapping of the clad region was also carried out to confirm the distribution of various elements. The results showed the presence of O, C, Cr, Ni, W, and Fe. The presence of Fe in the clad region supported and verified the claim of metallurgical bonding among the clad region and substrate region.

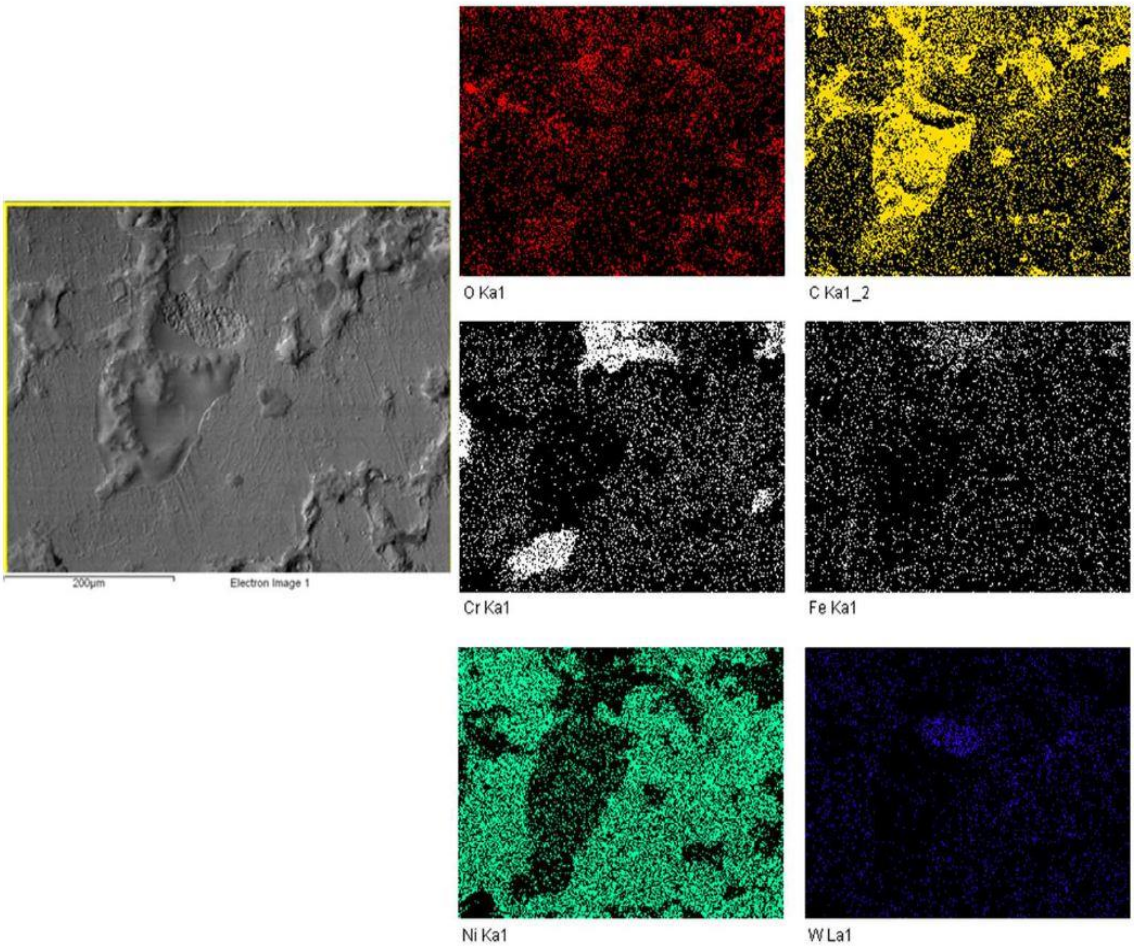

Figure 6.3: EDS area mapping of Ni-based10WC8Co-10Cr3C2 composite cladding

6.2.3 Microstructure Analysis of Ni-based20WC8Co-10Mo cladding

The back scattered image (BSE) image of the cross section of the developed Ni-based20WC8Co-10Mo clad is shown in figure 6.4 which discloses that the thickness of the clad is approximately 1.02 mm. The clad was free from any type of solidification cracks, major porosity, and interfacial cracks. After the MHH, the cladding was kept to solidify in the ambient temperature. The gaseous velocity of bubbles being formed in the molten metal during microwave processing of clad is higher than the solidification velocity which gives the gases sufficient time to get escaped during solidification, resulting in the formation of crack-free clads. The magnified image of the clad region shows the presence of hard carbide particles randomly distributed in the clad region.

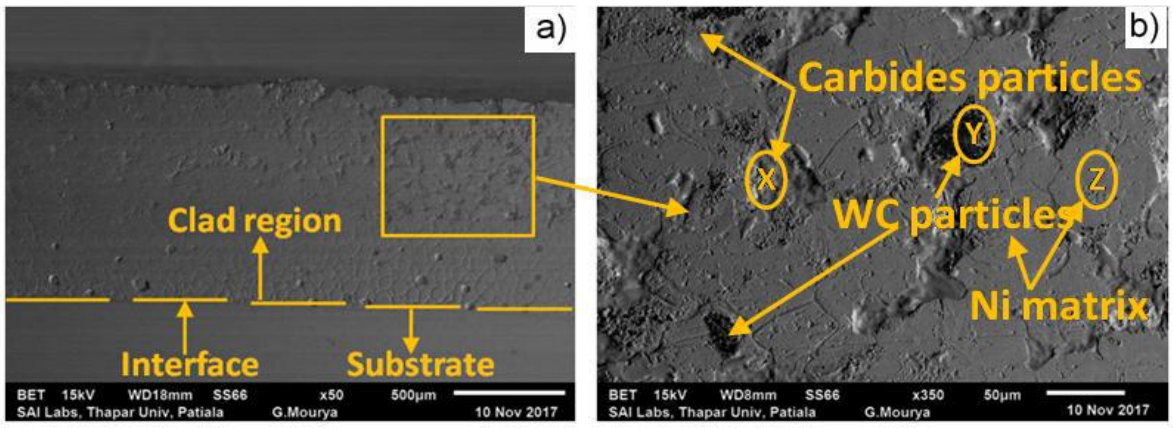

Figure 6.4: BSE image showing (a) cross section of clad (b) hard carbides and soft Nickel matrix region

6.2.4 Elemental study of Ni-based20WC8Co-10Mo cladding

The EDS analysis of BSE image of the clad region was also performed to confirm the presence of different elements. The results of EDS analysis shown in figure 6.5 revealed the existence of carbide particles in the majority at point X, the presence of W and C particles at point Y and at point Z Ni element was present in abundance.

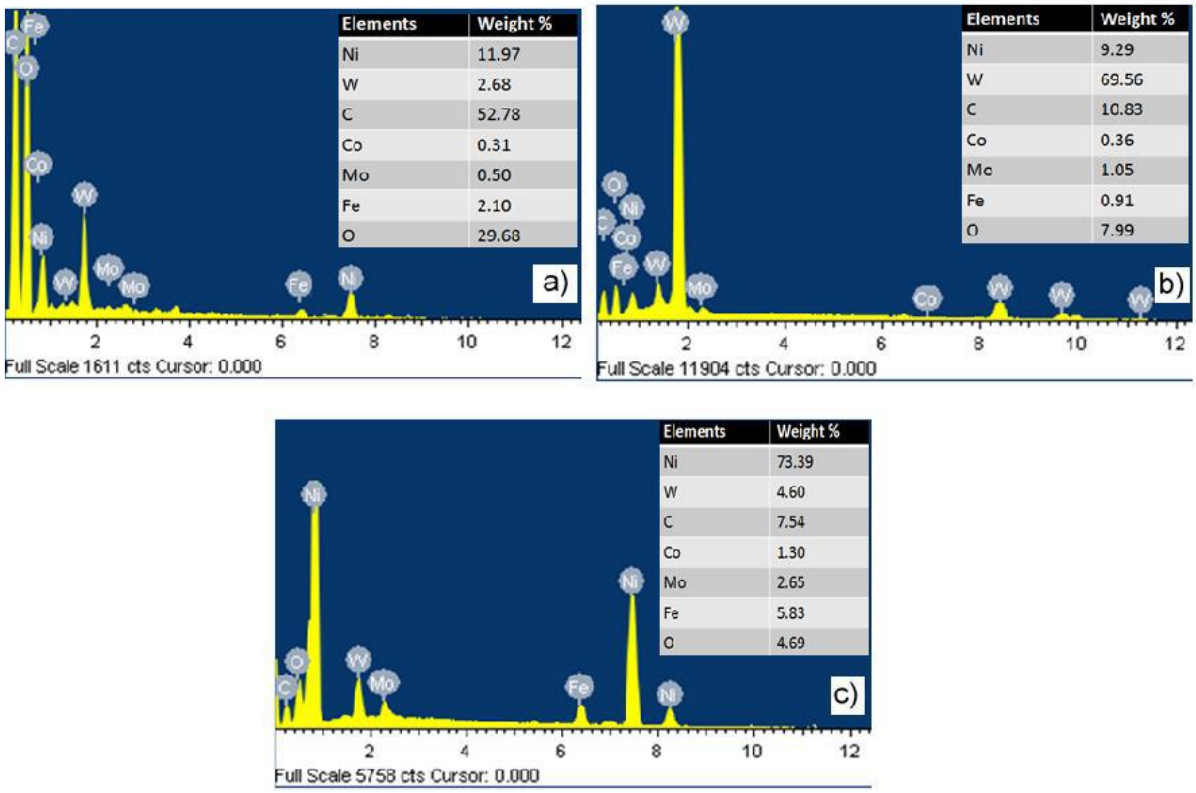

Figure 6.5: EDS analysis at (a) point X corresponding to figure 6.4(b), (b) point Y corresponding to
Figure 6.4 (b), and (c) point Z corresponding to figure 6.4 (b)

The area mapping of Backscattered electron composition image (BEC image) of the clad region was also carried out to know about the distribution of different elements and the results are displayed in figure 6.6. The presence of various elements such as C, O, Fe, Ni, W, Si, and Mo was confirmed by the results.

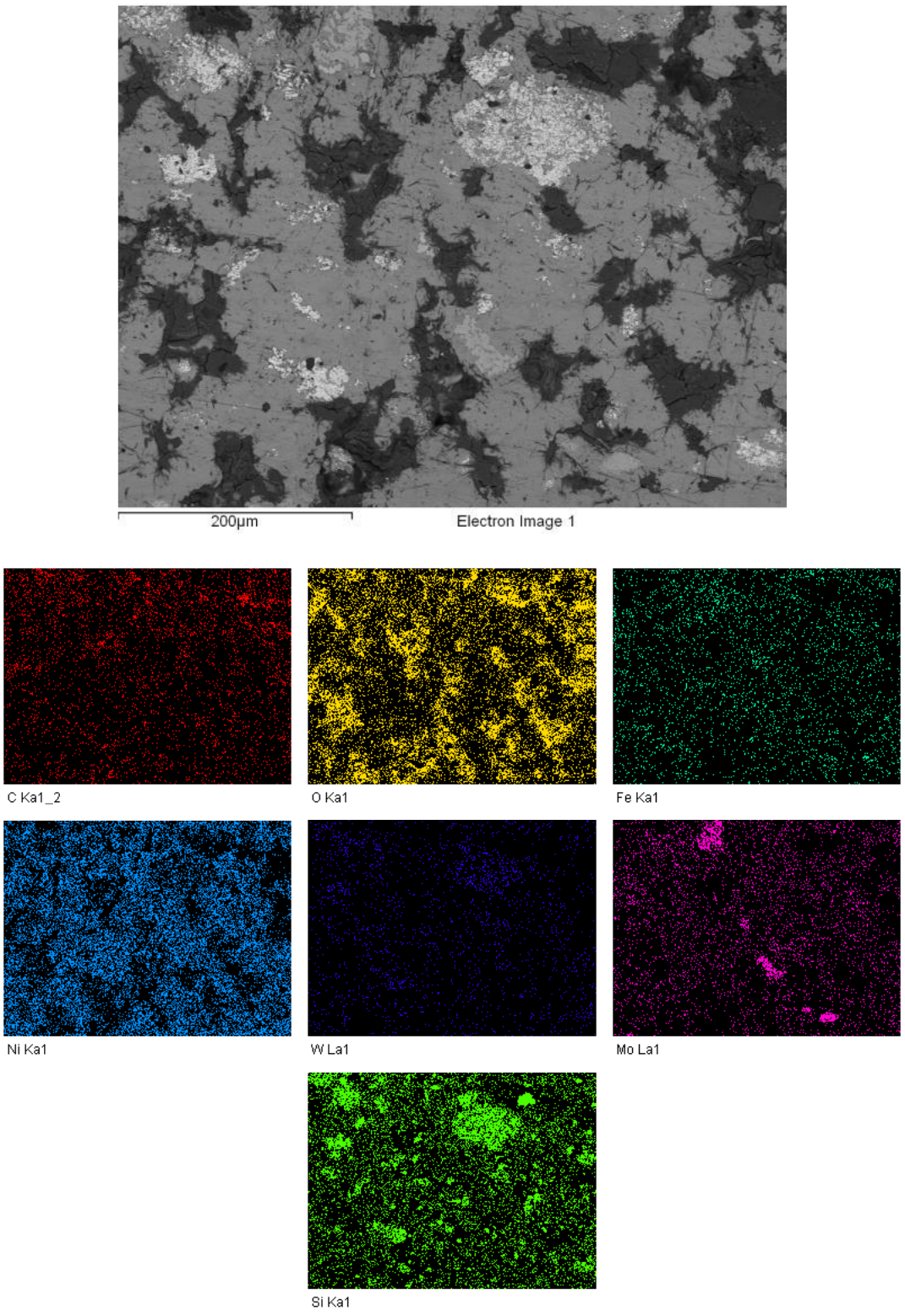

Figure 6.6: EDS area mapping of Ni-based20WC8Co-10Mo composite cladding

6.3 XRD analysis of composite clads

XRD analysis of both the composite clads was carried out in order to detect the presence of different phases during microwave processing of clads.

6.3.1 XRD of Ni-based10WC8Co-10Cr3C2 cladding

The XRD spectrum of the developed clad was carried out to confirm the presence of different phases in the clad region. The XRD detected the presence of phases such as $Co_3W_3C_4$, $FeNi_3$, Fe_6W_6C, Fe_7C_3, NiC, W_2C, Cr_7Ni_3, NiW, and Cr_7Ni_3 in the spectra. The presence of $FeNi_3$, Fe_6W_6C, and Fe_7C_3 in the clad region confirmed the formation of metallurgical bonding between the clad and substrate. The WC8Co particles break into free W and W_2C phases, which further reacts with free C to form $Co_3W_3C_4$. On the other hand, Cr_3C_2 particles break into Cr and C elements, which further reacts with Ni to form Cr_7Ni_3. NiW and NiC are formed owing to the reaction between C and W with Ni at a higher temperature.

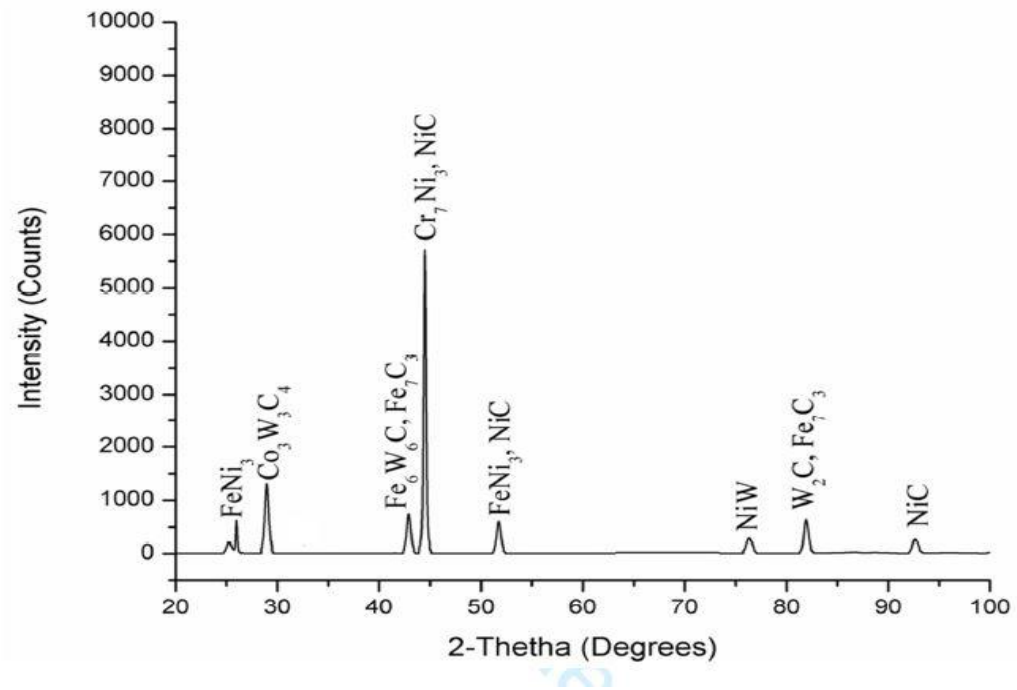

Figure 6.7: XRD spectra of Ni-based10WC8Co-10Cr3C2 composite cladding

6.3.2 XRD of Ni-based20WC8Co-10Mo cladding

The XRD spectra of the developed clad are shown in figure 6.8. The results of the spectra disclose the existence of Ni_4W, $NiSi_2$, Ni_2Mo_4C, Co_7Mo_6, Fe_3W_3C, $FeNi_3$, Mo_3Co_3 and W_2C phases in the clad region. During the heating of the clad in the microwave, WC particles break into free W and C. This free W and C particles react with Mo and Ni to form Ni_4W and

Ni_2Mo_4C. At higher temperature during heating of the clad, Ni and Si react to form $NiSi_2$. The presence of phases like Fe_3W_3C, $FeNi_3$ approves the limited dilution of Fe elements to the clad region from the substrate. The presence of Ni_2Mo_4C, Fe_3W_3C, and W_2C phases is a good indication of anti-wear cladding, which also aids the increase in the value of microhardness of the composite clad.

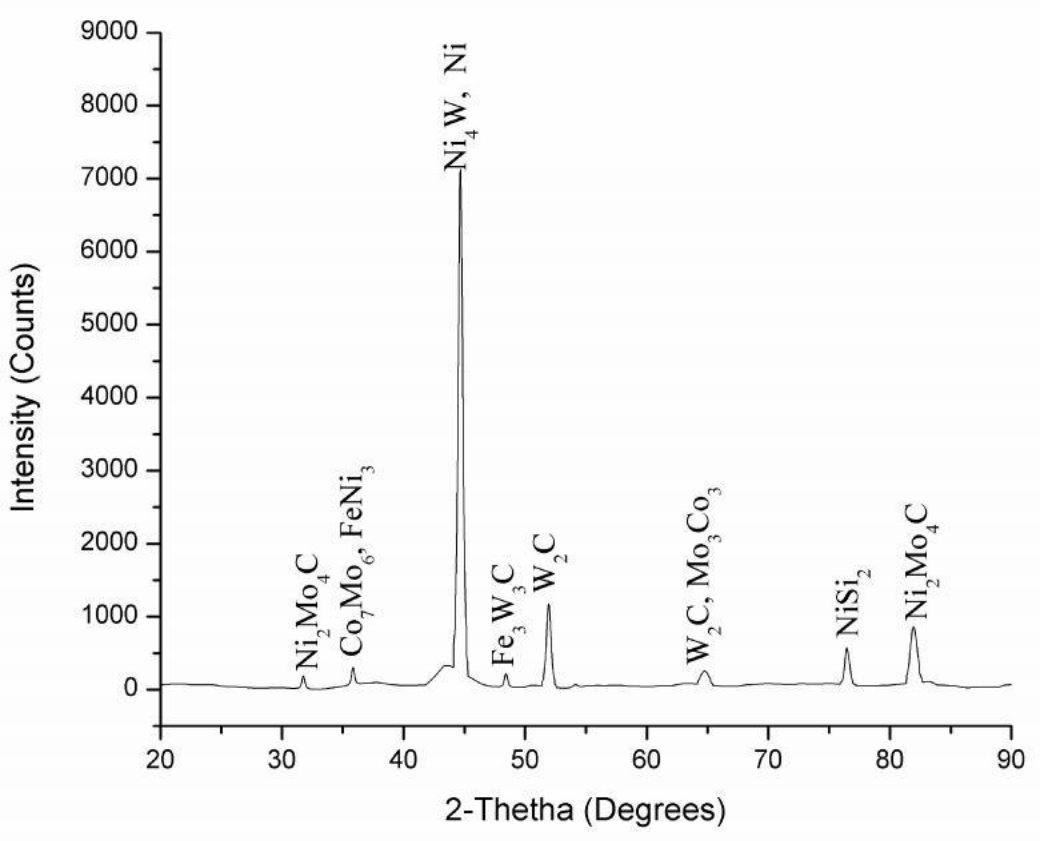

Figure 6.8: XRD spectra of Ni-based20WC8Co-10Mo composite cladding

6.4 Microhardness

Vickers microhardness tester was used to measure the microhardness of both the developed clads. The measurement of microhardness was carried out at intervals of 150 µm while moving from top layer of the clad to the substrate region.

6.4.1 Microhardness of Ni-based10WC8Co-10Cr3C2 cladding

Microhardness is a crucial parameter which directly influences the wear resistance of the material. The existence of Fe_6W_6C, Fe_7C_3, NiC, W_2C and $Co_3W_3C_4$ phases inside the microwave clad helps to increase the microhardness of the clad portion. The microhardness test was performed on the developed clads at the interval of 140 µm starting from the top of the clad towards the substrate region, to verify the fact that hard carbides present in the clad region increase the microhardness of the clad. It was witnessed that the value of average microhardness

in the clad region was 503 ± 34 Hv, the value decreased to 402 ± 76 Hv while approaching towards interface region as shown in figure 6.9. The existence of hard carbide phases and soft Ni matrix in the clad region leads to enormous standard deviation in the microhardness readings. It was noticed that indent in the carbide phase region showed small deformation leading to high microhardness value of carbide phase, whereas indent in the soft Ni matrix showed large deformation leading to a low value of microhardness.

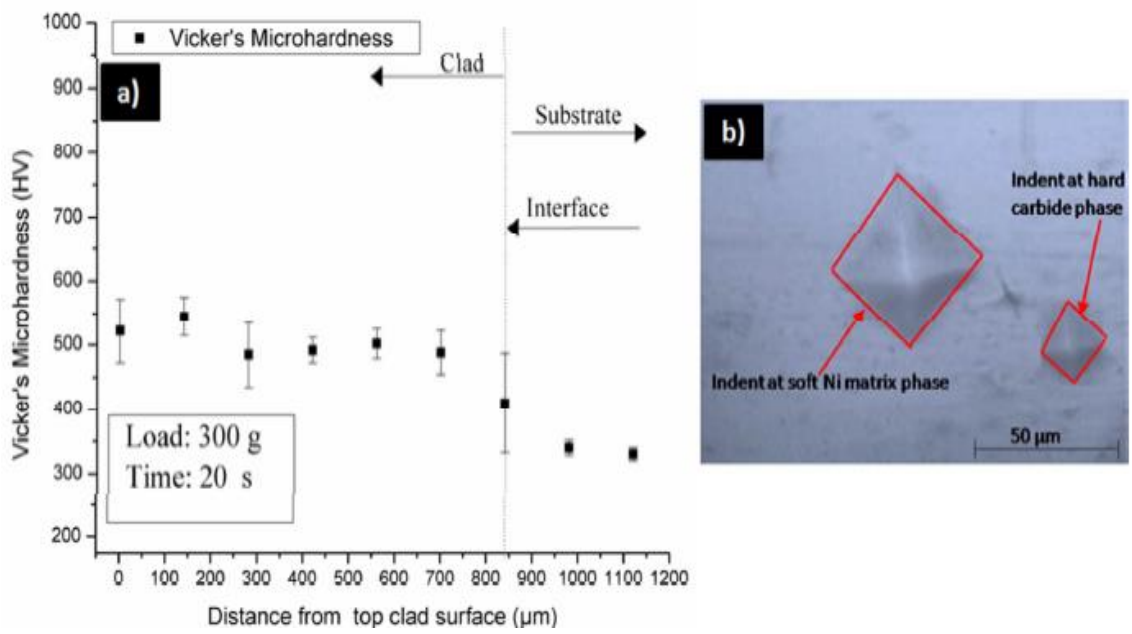

Figure 6.9: (a) Microhardness values of developed clad at different locations, (b) Optical Microscope image of microhardness indentation morphology

6.4.2 Microhardness of Ni-based20WC8Co-10Mo cladding

The microhardness test of the developed composite clads was performed to verify the fact that presence of hard carbide phases like Ni_2Mo_4C, Fe_3W_3C and W_2C increases the microhardness of the clad. The indents were taken at a gap of 170 µm in the clad region beginning from the top of the clad. Three readings were noted at each level. The load was set to 300 g and dwell time was fixed at 20 s for all the readings. It was witnessed that the average value of microhardness at the top of clad was 752 ± 34 Hv and at the interface region, microhardness that was recorded was 421 ± 85 Hv. The microhardness in the clad region was 2.5 times more than that of SS-316 L substrate. The large standard deviation that can be seen in the readings is due to the existence of hard carbide phases as well as soft Ni matrix simultaneously in the clad region.

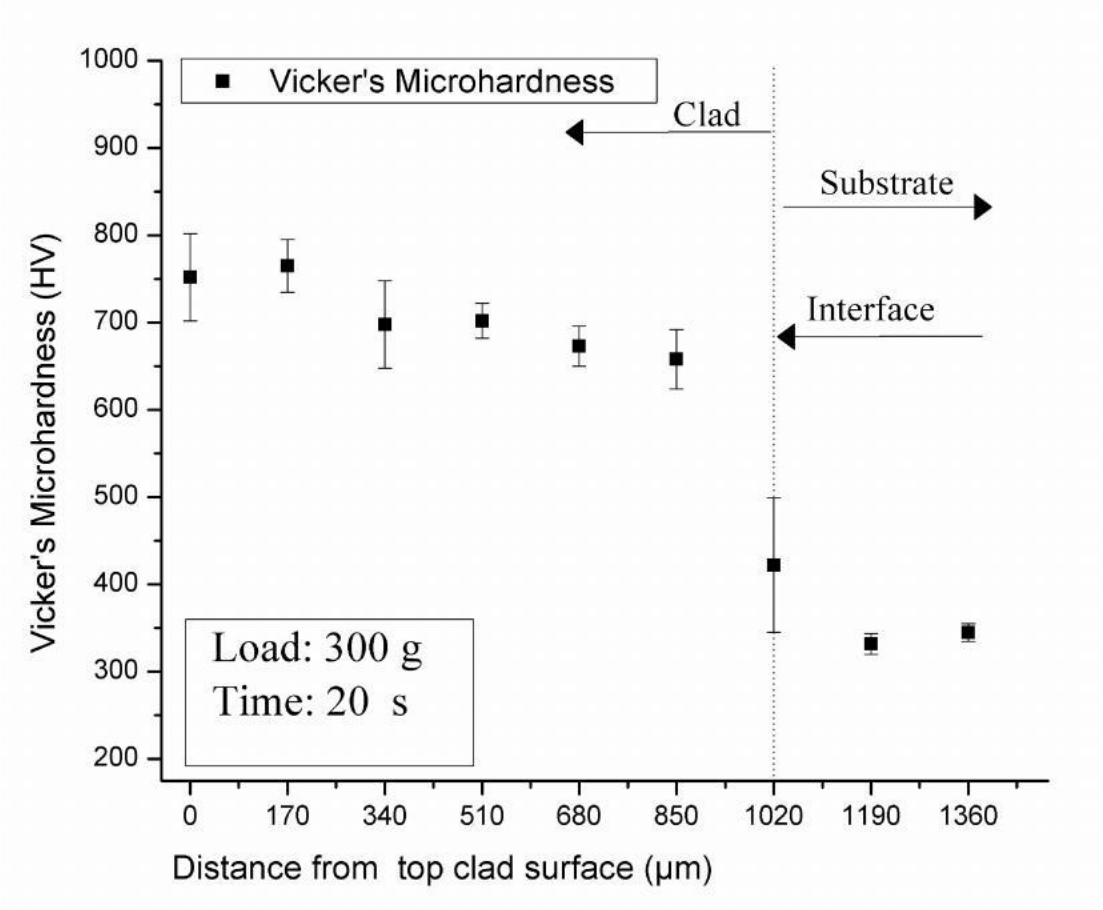

Figure 6.10: Distribution of Vickers microhardness across a typical section of Ni-based20WC8Co-10Mo clad

6.5 Flexural Strength

Flexural strength is one of the key mechanical property of the components. In the present work, flexural strength test of the developed clads of Ni-based20WC8Co-10Mo and Ni-based10WC8Co-10Cr3C2 was performed using three-point bend test as explained in chapter 4. The average value of maximum deformation (mm), load (kN) and calculated flexural strength (MPa) is shown in table 6.1. The graph of both the clads was divided into three different stages as shown in figure 6.11 and 6.12.

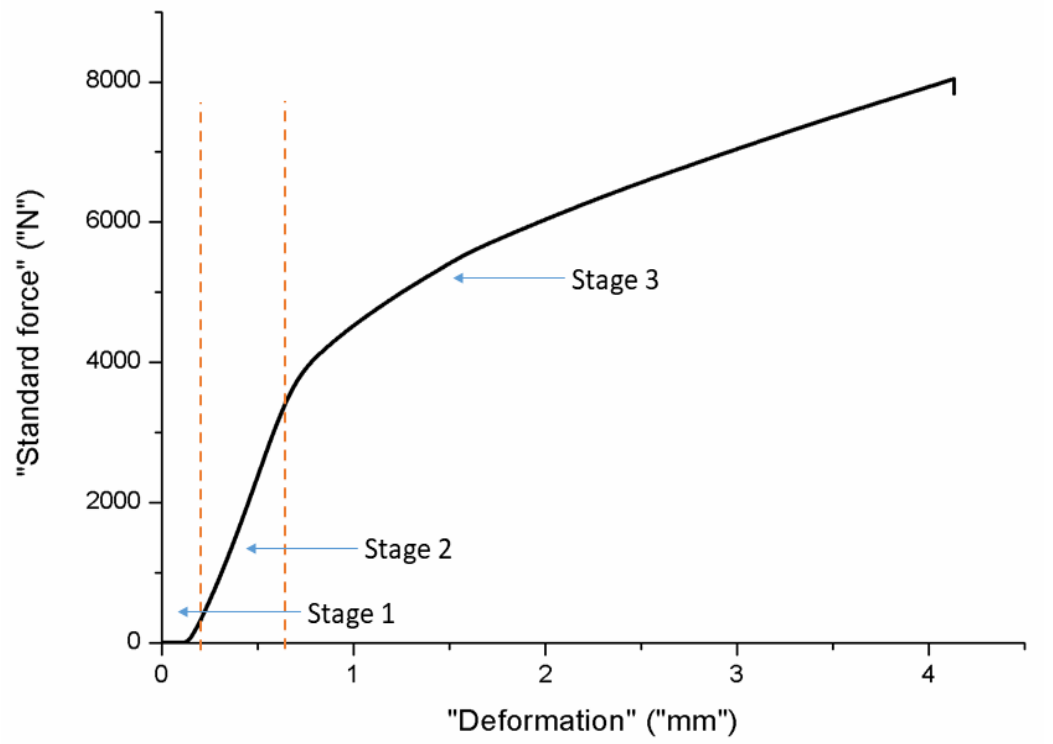

Figure 6.11: Load vs deformation graph of flexural strength test of Ni-based20WC8Co-10Mo clad during three-point bend test

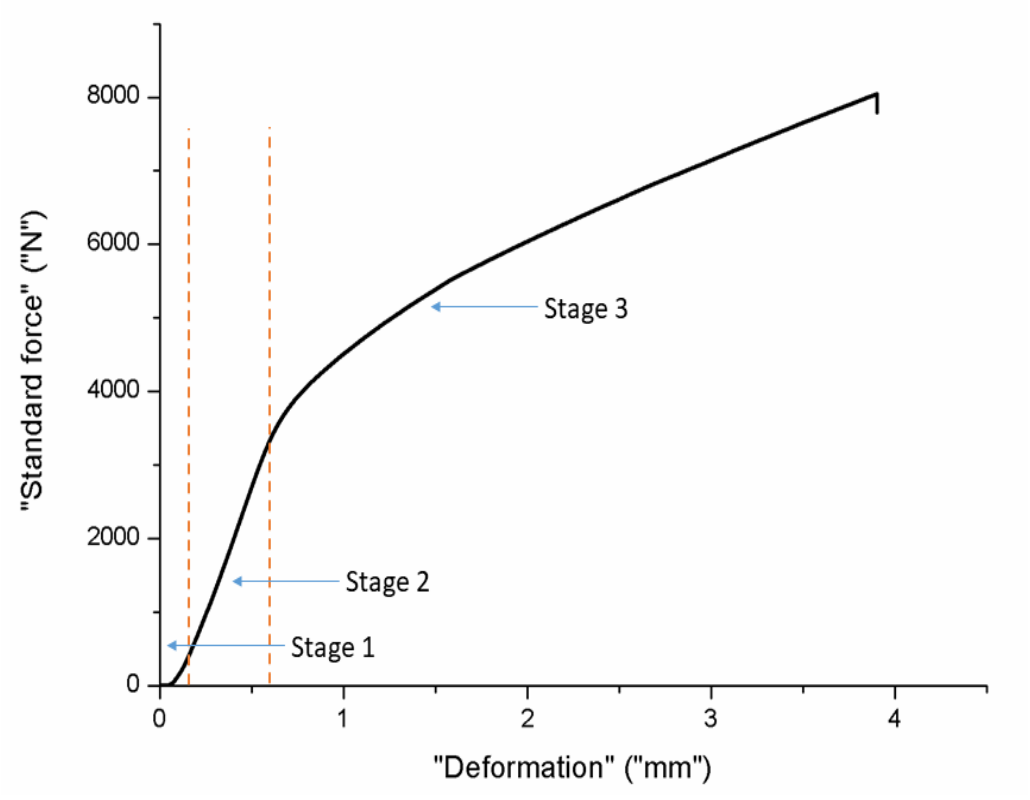

Figure 6.12: Load vs deformation graph of flexural strength test of Ni-based10WC8Co-10Cr3C2 clad during three-point bend test

During stage 1, uniform load deformation behaviour was observed up to ~ 200 N of the load for Ni-based20WC8Co-10Mo clad and up to ~ 150 N of the load for Ni-based10WC8Co-10Cr3C2 clad. Further, in stage 2, there was a sharp increase in load from ~ 200 N to ~ 3750 N with a deformation of 0.60 mm for Ni-based20WC8Co-10Mo clad, and from ~ 150 N to ~ 3600 N with a deformation of 0.55 mm for Ni-based10WC8Co-10Cr3C2 clad. Till stage 2 elastic limit of the clads continues and micro cracks were observed on the top of both the clads. During this stage, plastic deformation in the clads just starts as the hard carbides in the clads takes the load and show a sharp increase in load deformation characteristics. The minor cracks which were formed in stage 2 propagate as the load increases and turn into a major crack in stage 3 as shown in figure 6.13. During stage 3, more plastic deformation in the clads occur and the clads gets failed with an increase in load as the load is shifted to the SS-316 L substrate.

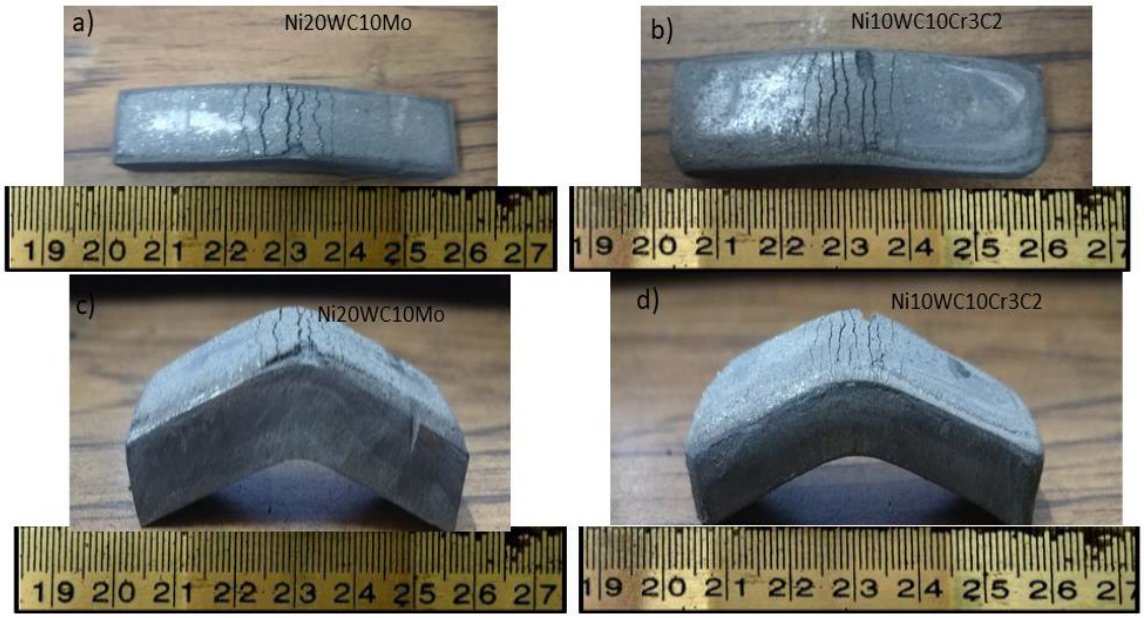

Figure 6.13: Picture of fractured specimens of microwave processed clads a) top view of Ni-based20WC8Co-10Mo clad, b) top view of Ni-based10WC8Co-10Cr3C2 clad, c) side view of Ni-based20WC8Co-10Mo clad, d) side view of Ni-based10WC8Co-10Cr3C2 clad

Table 6.1: Flexural strength of the developed microwave cladding

Microwave Cladding	Maximum load (kN)	Maximum displacement (mm)	Maximum flexural strength (MPa)
Ni-based20WC8Co-10Mo	8.056	4.13	834
Ni-based10WC8Co-10Cr3C2	7.645	3.90	797

6.6 Wear Study

The pin-on-disc tribometer was used to determine the wear rate of the microwave processed clads under different testing parameters. The effect of sliding velocity and sliding distance on cumulative weight loss was studied and discussed in the following sections. The fractographic analysis of Ni-based20WC8Co-10Mo and Ni-based10WC8Co-10Cr3C2 clads and SS-316 L substrate were also carried out to know about the wear mechanism during dry sliding.

6.6.1 Tribological study of SS-316 L

Austenitic stainless steel (SS-316 L) is known for its high strength, high corrosion resistance, and easy availability, but SS-316 L shows poor wear resistance characteristics under severe conditions. The sliding wear test of SS-316 L substrate was carried out on a pin-on-disc tribometer. The cumulative weight loss vs sliding distance graph is shown in figure 6.14. The weight loss at 2 kg of the normal load is quite significant and failure of the component can occur.

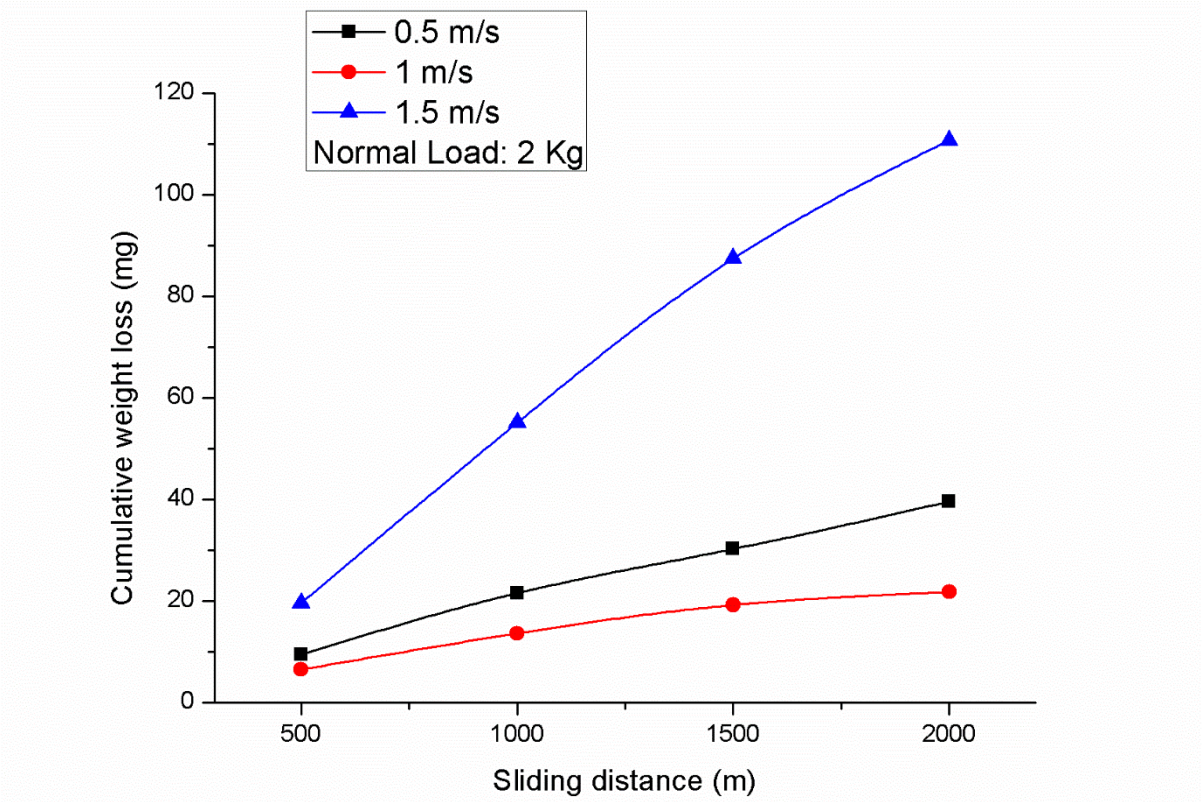

Figure 6.14: Cumulative weight loss vs sliding distance graph of SS-316 L substrate at different sliding velocities and 2 kg normal load

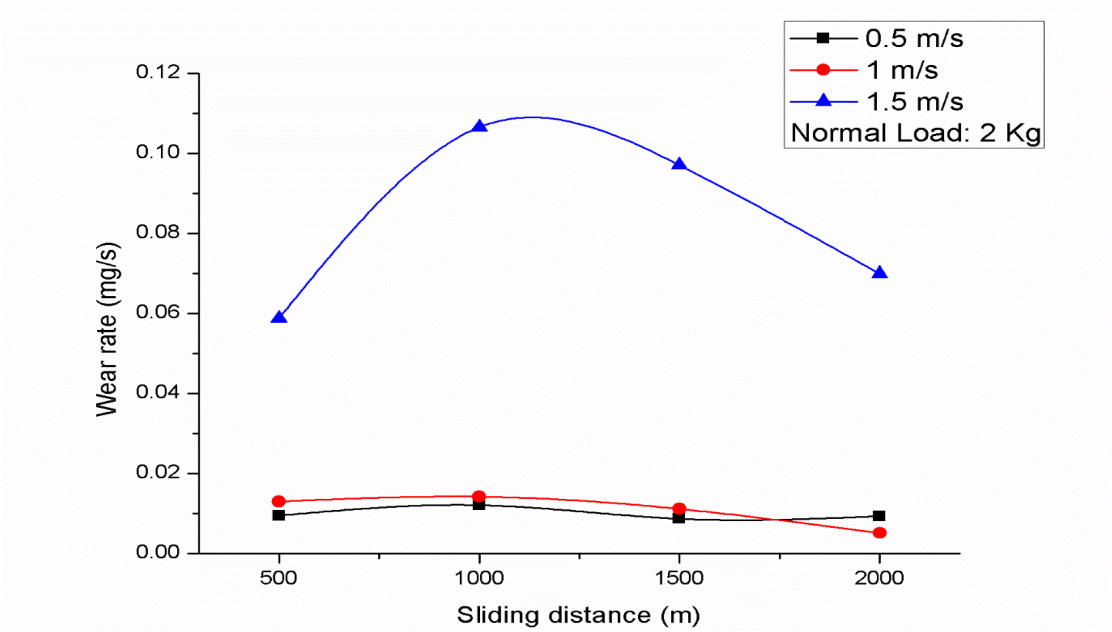

Figure 6.15: Wear rate characteristics of SS-316 L substrate

Fractographic analysis of worn material

The microstructure of the worn out sample of SS-316 L shows the sign of shearing, plastic deformation and crater formation as shown in figure 6.16. During sliding at lower and medium velocity, the removal of material is primarily due to plastic deformation trailed by the formation of craters. At higher sliding velocity, there is substantial plastic flow trailed by shearing of the material surface as shown in figure 6.16 (c).

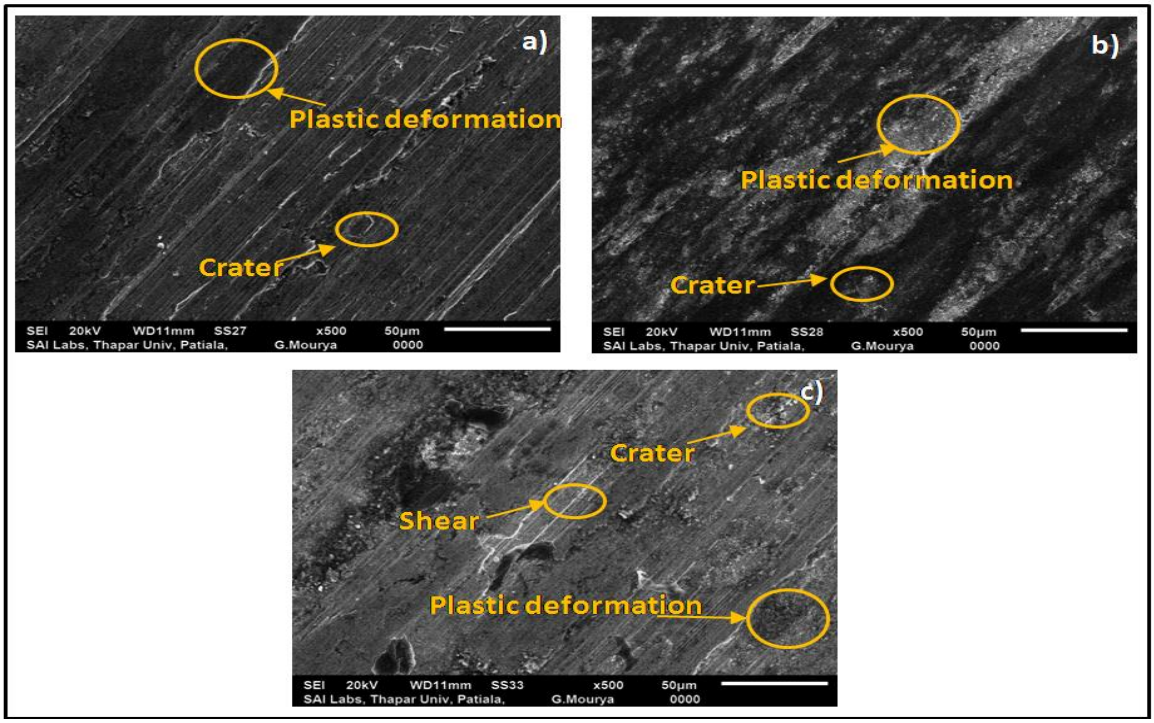

Figure 6.16: SEM images of worn out samples of SS-316 L substrate at 2 kg normal load and sliding velocity of a) 0.5 m/s, b) 1 m/s and c) 1.5 m/s at the end of 2000 m sliding distance

6.6.2 Tribological study of Ni-based10WC8Co-10Cr3C2 cladding

The developed clads of Ni-based10WC8Co-10Cr3C2 was tested for wear performance on a pin-on-disc tribometer. The weight loss of the clads was measured with respect to different sliding velocities and normal load conditions. The different set of parameters that were used during the experiment are discussed in table 5.2. The cumulative weight loss graph is shown in figure 6.18. The following section discusses the effect of varying sliding velocity and normal load conditions on weight loss.

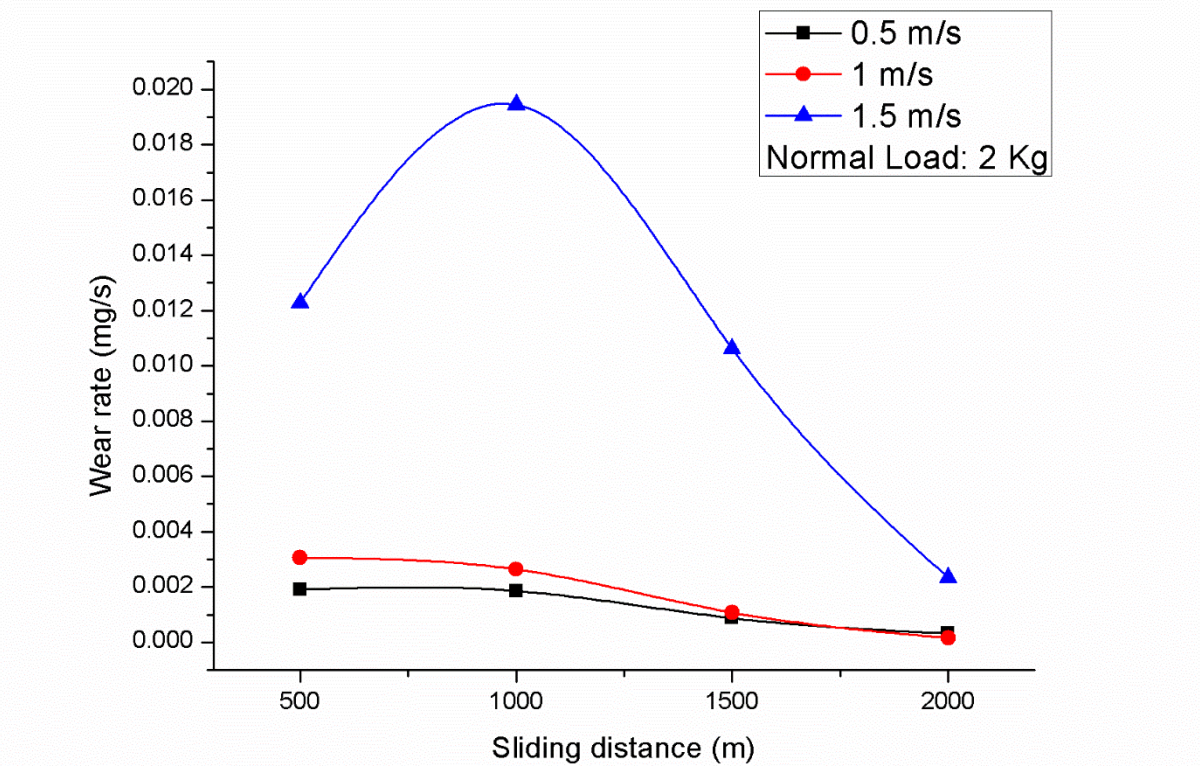

Figure 6.17: Wear rate characteristics of clad at 2 kg normal load

Influence of sliding velocity on weight loss

The sliding velocity of 0.5, 1 and 1.5 m/s was selected for determining the weight loss of the developed clads. The figure 6.18 shows that the cumulative weight loss decreases with increase in sliding velocity. The highest weight loss was recorded at 1.5 m/s sliding velocity and it was interesting to find out that the weight loss at 1 m/s was lower than the weight loss at 0.5 m/s sliding velocity. This may be credited to the development of an unstable oxide layer, also known as tribo layer, during chafing of surfaces in contact at a moderate velocity which tends to resist the wear, but the film formation is for short period only and gets smeared during further sliding.

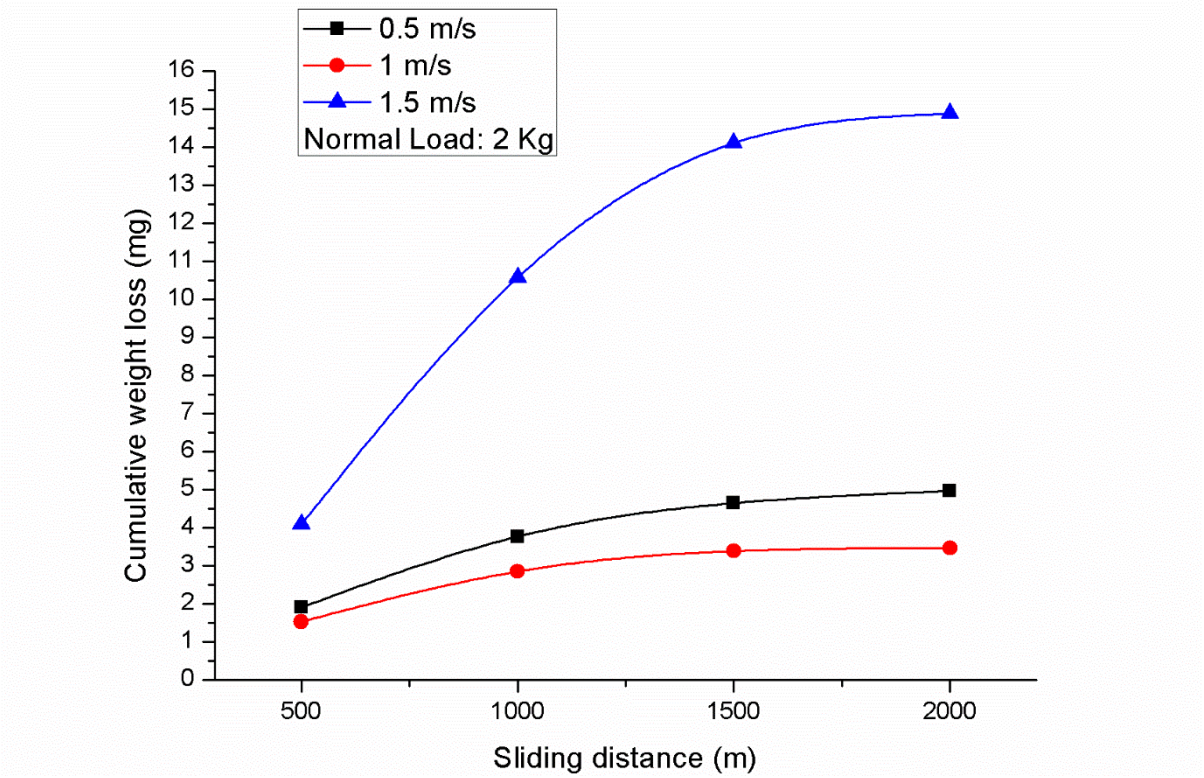

Figure 6.18: Cumulative weight loss vs sliding distance graph of Ni-based10WC8Co-10Cr3C2 clad at different sliding velocities and 2 kg normal load

Influence of sliding distance on weight loss

It was observed from the figure 6.18 that the weight loss slopes were steep up to a sliding distance of 1000 m. This was due to the existence of rough surface asperities in the initial run-in wear phase. However, the slope started to flatten after wear pin slide 1000 m of distance due to the achievement of a semi-steady state of wear. On the contrary, the wear rate starts to increase with an increase in normal load resulting in the removal of binder and disintegration of carbide grains. The weight loss for initial 500 m sliding distance was higher at the normal load of 2 Kg because of high friction and heat generation between the mating surfaces leading to surface micro-weldment.

Fractographic analysis of worn material

The wear behaviour of the surfaces in contact was studied by doing the fractographic analysis. The SEM images of the worn out sample of the clads is shown in figure 6.19. The formation of craters and grooves can easily be seen on the sliding surfaces. The formation of craters at the moderate velocity can be attributed to the material debonding and carbide pull out. At the higher velocity, the time period of the contact of sliding surfaces is shorter but the heat generation is more because of higher velocity, therefore plastic deformation is mainly responsible for the loss

of material followed by shearing of the clad surface. The smeared oxide layer can easily be seen in the figure 6.19 (a). The worn debris of the clad was also analyzed through SEM/EDS as shown in the figure 6.20.

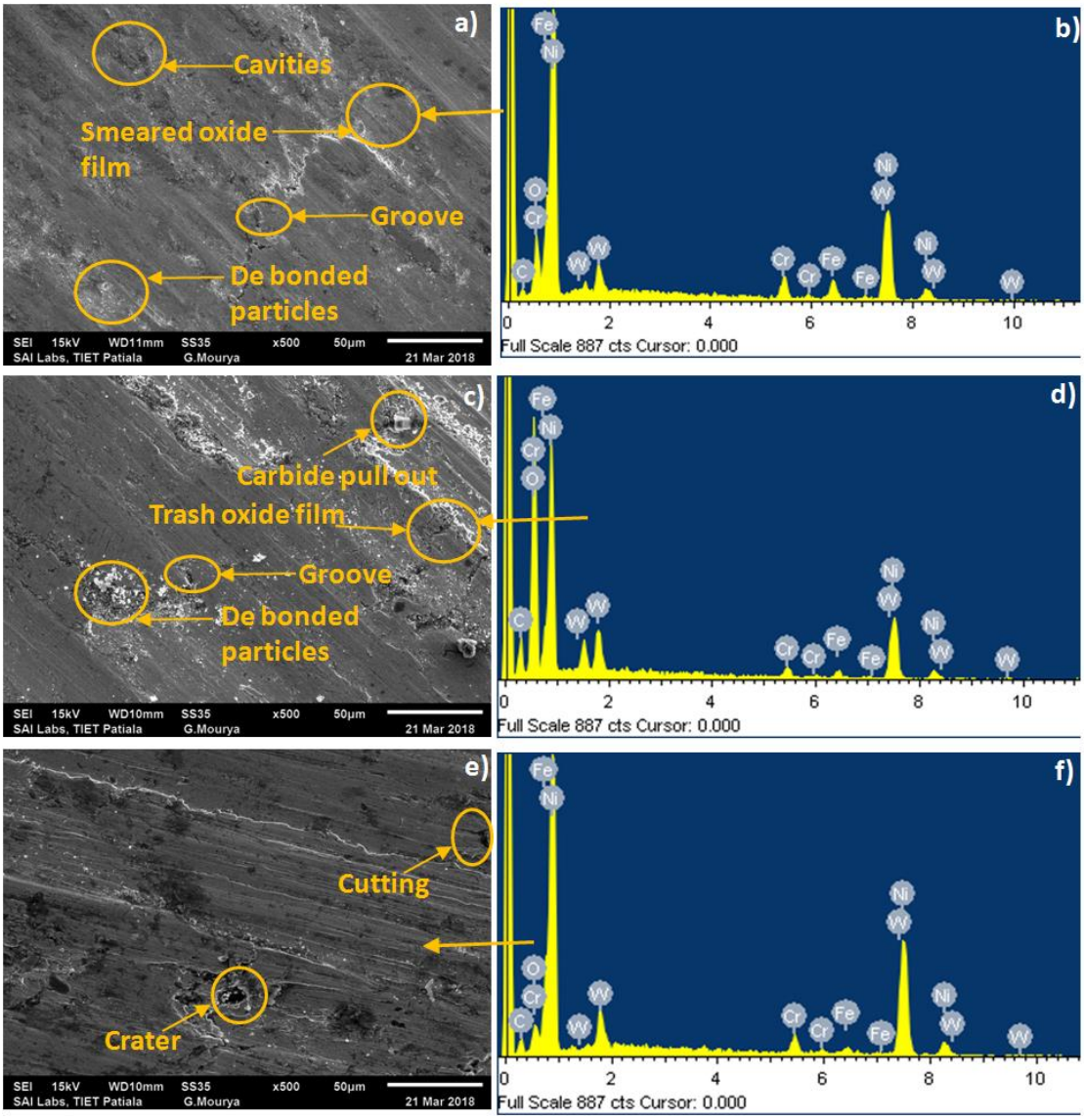

Figure 6.19: SEM images of worn out samples of Ni-based10WC8Co-10Cr3C2 clads at 2 kg normal load and sliding velocity of a) 0.5 m/s, c) 1 m/s and e) 1.5 m/s at the end of 2000 m sliding distance; b), d) and f) EDS analysis of wear debris

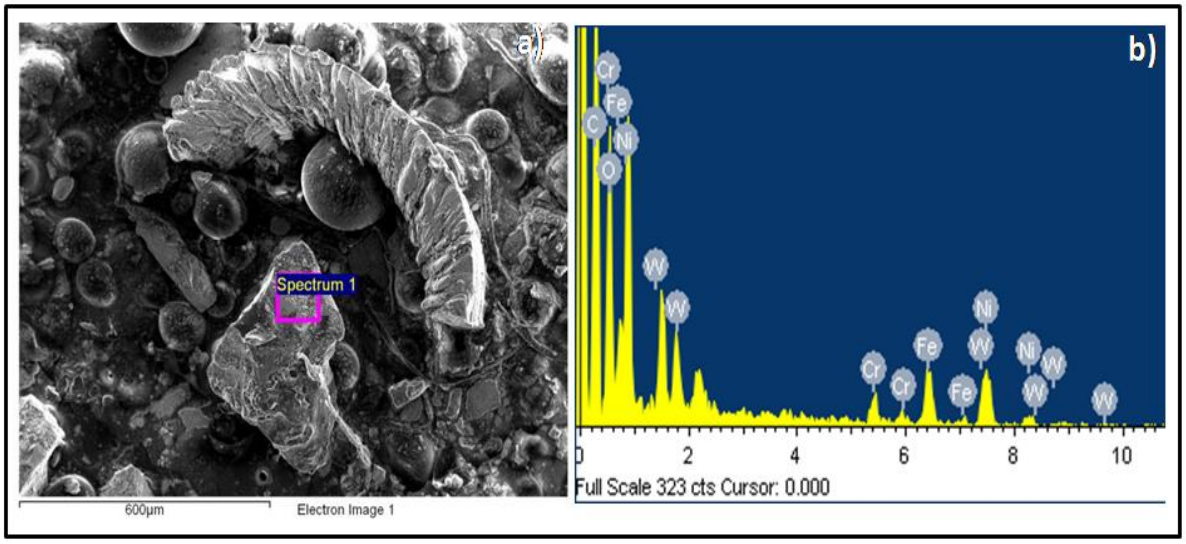

Figure 6.20: a) SEM images of debris during wear test collected after 2000 m of sliding distance of Ni-based10WC8Co-10Cr3C2 clad, b) EDS analysis of wear debris

6.6.3 Tribological study of Ni-based20WC8Co-10Mo cladding

A pin-on-disc tribometer was used to perform dry sliding wear test of Ni-based20WC8Co-10Mo clad where the clad face (wear pin) was rubbed against alumina disc under different testing parameters as shown in table 5.2. The cumulative weight loss vs sliding distance graph at a normal load of 2 Kg is shown in the figure 6.22. It was observed that the cumulative weight loss of clad was significantly lesser than the SS-316 L samples. The study of dry sliding wear has been carried out in systematic way and influence of sliding distance and sliding velocity including fractographic analysis has been discussed in subsequent section. Wear rate characteristics are shown in figure 6.21.

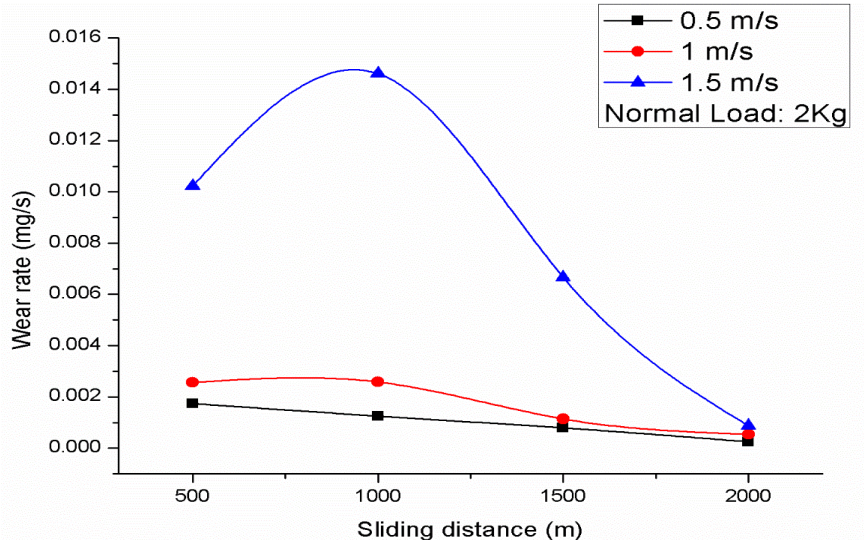

Figure 6.21: Wear rate characteristics of clad at 2 kg normal load

Influence of sliding velocity on weight loss

The sliding velocity plays a vital role in the wear process especially when the two surfaces are rubbing against each other in dry condition and at room temperature. The highest weight loss was recorded at 1.5 m/s sliding velocity and it was interesting to find out that the weight loss at 1 m/s was lower than the weight loss at 0.5 m/s sliding velocity. This may be credited to the development of an unstable oxide layer, also known as tribo layer, during chafing of surfaces in contact at a moderate velocity which tends to resist the wear, but the film formation is for short period only and gets smeared during further sliding. The weight loss is more at 0.5 m/s sliding velocity because oxide layer formation is deferred due to a lower temperature at lower sliding velocity. On the same note, the temperature rise at 1.5 m/s sliding velocity reaches an extent that the oxide layer gets shattered.

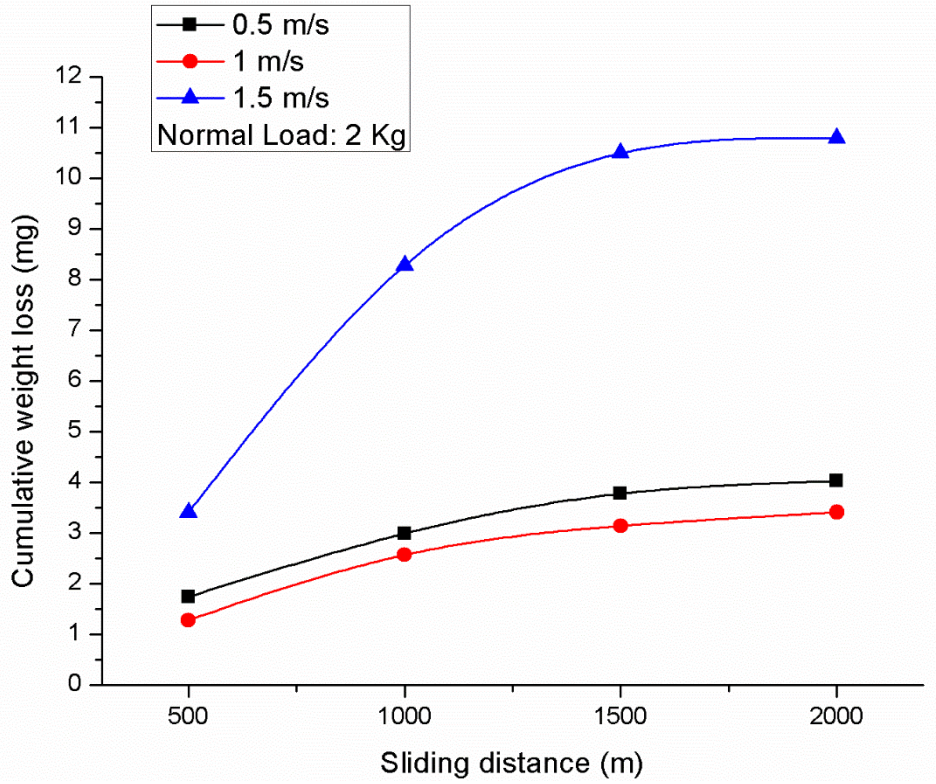

Figure 6.22: Cumulative weight loss vs sliding distance graph of Ni-based20WC8Co-10Mo clad at different sliding velocities and 2 kg normal load

Influence of sliding distance on weight loss

It was observed from the figure 6.22 that the weight loss slopes were steep up to a sliding distance of 1000 m. This was due to the existence of rough surface asperities in the initial run-in wear phase. However, the slope started to flatten after 1000 m of sliding distance due to the achievement of a semi-steady state of wear. On the contrary, the wear rate starts to increase

with an increase in normal load resulting in the removal of binder and disintegration of carbide grains. The weight loss for initial 500 m sliding distance was higher at the normal load of 2 Kg because of high friction and heat generation between the mating surfaces leading to surface micro-weldment.

Fractographic analysis of worn material

The SEM images of fractographic analysis of a worn out sample of Ni-based20WC8Co-10Mo clad are shown in figure 6.23. The image in figure 6.23 (a) shows that the clad suffers from defects like cavities, groove and minor de bonded particles at a medium sliding velocity of 1 m/s. At higher sliding velocity i.e. 1.5 m/s, the primary damage occurred due to high plastic deformation followed by shearing of the displaced material, leading to a lesser loss in weight of clad material as compared to the loss in weight at lower and medium sliding velocities.

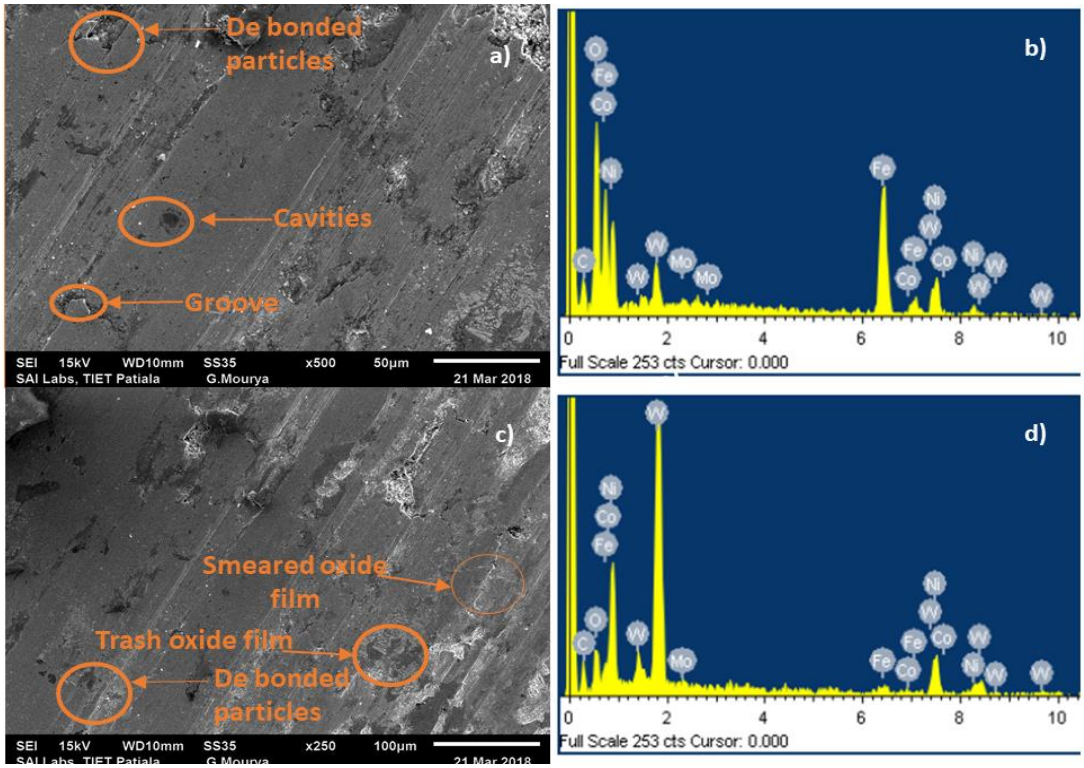

Figure 6.23: SEM images of worn out samples of Ni-based20WC8Co-10Mo clads at 2 kg normal load and sliding velocity of a) 0.5 m/s, b) 1 m/s and c) 1.5 m/s at the end of 2000 m sliding distance

6.7 Reduction in Wear

The comparison of weight loss of developed clads and substrate sample is shown in figure 6.24. It can be concluded that the weight loss of the developed clads is significantly less than SS-316 L substrate. The lower weight loss of the microwave processed clads was due to the formation

of hard carbides which increases the wear performance of the clads. The weight loss in case of SS-316 L substrate is 110.81 mg which is 7.5 times more than the weight loss of Ni-based10WC8Co-10Cr3C2 clad and 10.3 times more than the weight loss of Ni-based20WC8Co-10Mo clad.

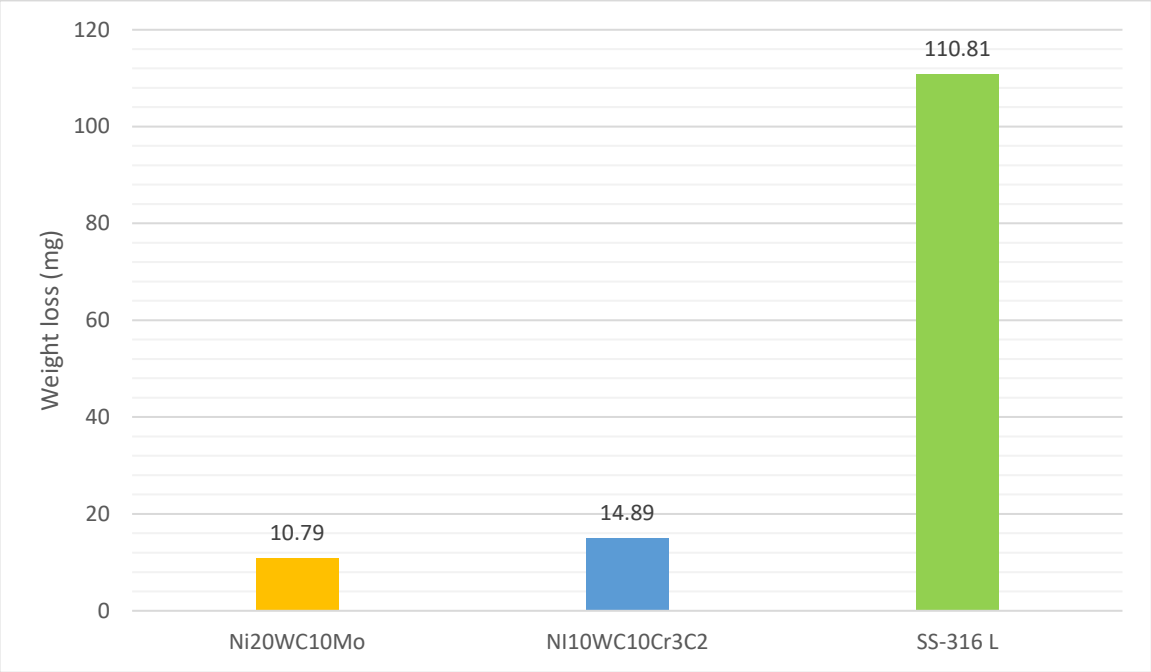

Figure 6.24: Comparison of weight loss between the developed clads and SS-316 L substrate at 1.5 m/s sliding velocity and 2 kg of normal load

Chapter 7
Conclusion and Future Scope

7.1 Conclusion

In the present study, the work was mainly focussed on the development of wear resistant composite cladding of Ni-based10WC8Co-10Cr3C2 and Ni-based20WC8Co-10Mo powders on SS-316 L substrate through microwave hybrid heating technique. The developed clads were characterized by various relevant methods, the major conclusions drawn from the present work are as follows:

1. The microstructure from the SEM images revealed that the clads of approximately 1 mm thickness were developed on SS-316 L substrate through microwave hybrid heating technique.
2. The developed clads were free from any type of interfacial and solidification cracks, major porosity, and voids.
3. XRD of Ni-based10WC8Co-10Cr3C2 clad revealed the presence of phases such as $Co_3W_3C_4$, $FeNi_3$, Fe_6W_6C, Fe_7C_3, NiC, W_2C, Cr_7Ni_3, NiW and Cr_7Ni_3 in the spectra whereas XRD of Ni-based20WC8Co-10Mo clad showed the presence of Ni_4W, $NiSi_2$, Ni_2Mo_4C, Co_7Mo_6, Fe_3W_3C, $FeNi_3$, Mo_3Co_3 and W_2C phases in the clad region.
4. The presence of hard carbides particles such as Fe_6W_6C, Fe_7C_3, NiC, W_2C and $Co_3W_3C_4$ phases inside the Ni-based10WC8Co-10Cr3C2 clad, and existence of phases like Ni_2Mo_4C, Fe_3W_3C and W_2C in Ni-based20WC8Co-10Mo clad are responsible for increase in microhardness of the developed clads, which was measured to be 503 ± 34 Hv for Ni-based10WC8Co-10Cr3C2 clad and 752 ± 34 Hv for Ni-based20WC8Co-10Mo clad.
5. The existence of phases like Fe_6W_6C, Fe_7C_3, Fe_3W_3C established the partial dilution of Fe elements in the clad region from the substrate and hence, confirmed the claim of metallurgical bonding in developed clad during microwave hybrid heating.
6. The average flexural strength of Ni-based20WC8Co-10Mo clad was 834 MPa whereas the flexural strength of Ni-based10WC8Co-10Cr3C2 clad was 797 MPa. Therefore, the flexural strength of Ni-based20WC8Co-10Mo clad was higher than the flexural strength of Ni-based10WC8Co-10Cr3C2 clad by approximately 5%.

7. The wear resistance of Ni-based20WC8Co-10Mo clad and Ni-based10WC8Co-10Cr3C2 clad was 10.3 times and 7.5 times higher than the wear resistance of substrate respectively.

7.2 Scope for future work

Various studies have been carried out on development and characterization of microwave processed clads, but still, a lot of scopes is left in improving the research work in the area of microwave processing of materials. Some of the suggestions for future work are listed below:

1. To study the cavitation erosion wear resistance of the microwave processed clads.
2. An industrial microwave oven can be used to develop the clads in order to reduce the processing time of the clads.
3. A mathematical equation can be made to find out the processing time required for developing a good bonded clad by keeping the microwave power level, dimensions of the specimen to be claded as the changing parameters.
4. To study the surface roughness of the developed clads.

Visible outputs

LIST OF PUBLICATIONS IN INTERNATIONAL JOURNALS (SCI/SCIE):

- S. Kaushal, **D. Singh**, D. Gupta, H.L. Bhowmick and V. Jain, Processing of Ni-based20WC8Co-10Mo based composite clads on austenitic stainless steel through microwave hybrid heating, Materials Research Express.
  Status: ***Published Online***
  Publisher: ***IOP Publishing Ltd.***
  Impact Factor: ***1.151***
- S. Kaushal, **D. Singh**, D. Gupta, H.L. Bhowmick and V. Jain, Processing of Ni-WC-Cr_3C_2 based metal matrix composite cladding on SS-316 L substrate through microwave irradiation, Journal of Composite Materials.
  Status: ***Accepted***
  Publisher: ***SAGE***
  Impact Factor: ***1.613***
- S. Kaushal, **D. Singh**, D. Gupta, H.L. Bhowmick and V. Jain, Wear resistance of austenitic 316L steel by microwave processed composite clads, Surface Engineering
  Status: Under review
  Publisher: ***Taylor & Francis***
  Impact Factor: ***1.978***

LIST OF PUBLICATIONS IN INTERNATIONAL CONFERENCE:

- **D. Singh**, S. Kaushal, D. Gupta, H.L. Bhowmick and V. Jain, On processing of Ni-WC8Co based composite clads on austenitic stainless steel through microwave energy. Presented at ICEMMM (International Conference on Engineering Materials, Metallurgy and Manufacturing) held in Feb, 2018 at SSN College of Engineering, Chennai. (**Best Paper Award**)
  Publisher: ***Springer***
- S. Kaushal, **D. Singh**, D. Gupta, V. Jain and H.L. Bhowmick, Surface modification of SS-316 L steel using microwave processed Ni/WC based composite clads. Presented at ICDEM (International Conference on Design, Materials and Manufacture) held in Jan, 2018 at NIT Karnataka, Surathkal.
  Publisher: ***AIP Conference Proceeding***
- S. Kaushal, **D. Singh**, D. Gupta and H.L. Bhowmick, On development and characterization of microwave processed Ni + 30% SiC based composite clads. Presented at ICCMMEMS (International Conference on Composite Materials: Manufacturing, Experimental Techniques, Modeling and Simulation) held in March, 2018 at LPU, Punjab.
  Status: ***Selected for publishing in Elsevier***

References

[1] K.H. Lo, F.T. Cheng C.T. Kwok, H.C. Man. Improvement of cavitation erosion resistance of AISI 316 stainless steel by laser surface alloying using fine WC powder, Journal of Surface and Coatings Technology 165 (2003) 258–267.

[2] D. Gupta, A. K. Sharma, Microwave cladding: A new approach in surface engineering, Journal of Manufacturing Processes 16 (2014) 176–182.

[3] S. Zhou, X. Zeng, Q. Hu, Y. Huang, Analysis of crack behavior for Ni-based WC composite coatings by laser cladding and crack-free realization, Applied Surface Science 255 (2008) 1646-1653.

[4] X. Lin, T.M. Yue, H.O. Yang, W.D. Huang, Microstructure and phase evolution in laser rapid forming of a functionally graded Ti-Rene88DT alloy, Acta materialia 54 (2006) 1901–1915.

[5] C. Bezencon, A. Schnell, W. Kurz, Epitaxial deposition of MCrAlY coatings on a Ni based superalloy by laser cladding, Scripta materialia 49 (2003) 705–709.

[6] R. Vilar and E.C. Santos, Structure of NiCrAlY coatings deposited on oriented single crystal super alloy substrates by laser cladding, Advanced Materials Research 278 (2011) 503–508.

[7] D. Gupta and A.K. Sharma, Development and microstructural characterization of microwave cladding on austenitic stainless steel, Surface Coatings Technology 205 (2011) 5147–5155.

[8] S. Kaushal, D. Gupta, HL. Bhowmick, Investigation of dry sliding wear behavior of composite cladding developed through microwave heating, Journal of Tribology 139 (2017) 1–9.

[9] S. Zafar and A.K. Sharma, On friction and wear behavior of WC-12Co microwave clad, Tribology Transactions 58 (2015) 584–591.

[10] D. Gupta and A.K. Sharma, On microstructure and flexural strength of metal–ceramic composite cladding developed through microwave heating, Applied Surface Science 258 (2012) 5583– 5592.

[11] S. Kaushal, V. Sirohi, D. Gupta, Processing and characterization of composite cladding through microwave heating on martensitic steel. Material: Design and applications (2015).

[12] M. Oghbaei, O. Mirzaee, Microwave versus conventional sintering: a review of fundamentals, advantages and applications. Journal of Alloys and Compounds 494 (2010) 175–189.

[13] R.J. Lauf, D.W. Bible, A.C. Johnson, C.A. Everliegh, 2 to 18 GHz broadband microwave heating systems, Microwave Journal Vol. 36 (1993) 24–27

[14] E.T. Thostenson, T. Chou, Microwave processing: fundamentals and applications, Composites 30 (1999) 1055–1071.

[15] S. Singh , D. Gupta , V. Jain & A.K. Sharma, Microwave Processing of Materials and Applications in Manufacturing Industries: A Review, Materials and Manufacturing Processes 30 (2015) 1–29

[16] C. Leonelli, P. Veronesi, L. Denti, A. Gatto, L. Iuliano, Microwave assisted sintering of green metal parts, Journal of Materials Processing Technology 205 (2008) 489–496.

[17] A.K. Sharma, S. Aravindhan, R. Krishnamurthy, Microwave glazing of alumina titania ceramic composite coatings, Materials Letters 50 (2001) 295–301.

[18] A.K. Sharma, R. Krishnamurthy, Microwave processing of sprayed alumina composite for enhanced performance, Journal of the European Ceramic Society 22 (2002) 2849–60.

[19] D. Gupta, A.K. Sharma, Development and microstructural characterization of microwave cladding on austenitic stainless steel, Surface & Coatings Technology 205 (2011) 5147-5155.

[20] Z. Huang, M. Gotoh, Y. Hirose, Improving sinter-ability of ceramics using hybrid microwave heating, Journal of Materials Processing Technology 209 (2009) 2446–2452.

[21] D.K. Agrawal, J. Cheng, Microwave sintering of commercial WC/Co based hard metal tools, European conference, Advances in hard materials production (1999) 175-182.

[22] J. Cheng, D. Agrawal, Y. Zhang, R. Roy, Microwave sintering of transparent alumina, Materials Letters 56 (2002) 587-592.

[23] D. Agrawal, Latest global developments in microwave materials processing, Materials Research Innovations, 14 (2010) 3-8.

[24] M.S. Srinath, A.K. Sharma, P. Kumar, A new approach to joining of bulk copper using microwave energy, Materials and Design 32 (2011) 2685–2694.

[25] L. Sextona, S. Lavina, G. Byrnea, A. Kennedy, Laser cladding of aerospace materials, Journal of Materials Processing Technology 122 (2001) 63–68.

[26] K.H. Lo, F.T. Cheng, C.T. Kwok, H.C. Man, Improvement of cavitation erosion resistance of AISI 316 stainless steel by laser surface alloying using fine WC powder, Surface and Coatings Technology 165 (2003) 258-267.

[27] F. Liu, C. Liu, X. Tao, S. Chen, Laser cladding of Ni-based alloy on copper substrate, Journal of University of Science and Technology 13 (2006) 329-332.

[28] J. Stella, E. Schuller, C, Hebing, O.A. Hamed, M. Pohl, D. Stover, Cavitation erosion of plasma-sprayed NiTi coatings, Wear 260 (2006) 1020-1027.

[29]M. Parco, L. Zhao, J. Zwick, K. Bobzin, E. Lugscheider, Investigation of HVOF spraying on magnesium alloys, Surface and Coating Technology 201 (2006) 3269-3274.

[30] D. Gupta, A.K. Sharma, Development and microstructural characterization of microwave cladding on austenitic stainless steel, Surface and Coating Technology 205 (2011) 5147-5155.

[31] D. Gupta, A.K. Sharma, Microwave cladding: A new approach in surface engineering, Journal of Manufacturing Process 16 (2014) 176-182.

[32] S. Zafar, A.K. Sharma, Development and characterization of WC-12Co microwave clad, Materials Characterization 96 (2014) 241-248.

[33] S. Zafar, A.K. Sharma, Investigations on flexural performance and residual stresses in nanometric WC-12Co microwave clads, Surface & Coatings Technology 291 (2016) 413–422.

[34] S. Singh, D. Gupta, V. Jain, Novel microwave composite casting process: Theory, feasibility and characterization, Materials and Design 111 (2016) 51-59.

[35] S. Kaushal, D. Gupta, H. Bhowmick, On microstructure and wear behaviour of microwave processed composite clad, Journal of Tribology (2017).

[36] S.M. Lingappa, M.S. Srinath, H.J. Amarendra, Melting of bulk non-ferrous metallic materials by microwave hybrid heating (MHH) and conventional heating: a comparative study on energy consumption, Journal of Brazilian Society of Mechanical Sciences and Engineering (2017).